

# **Reconstituting the pathway to mitochondrial division**

**A thesis submitted in partial fulfillment of the requirements of the degree of  
Doctor of Philosophy**

**by**

**Sukrut C Kamerkar**

**20122020**



**Indian Institute of Science Education and Research Pune**

**2019**

# CERTIFICATE

Certified that the work incorporated in the thesis entitled “Reconstituting pathway to mitochondrial division” submitted by Sukrut C Kamerkar was carried out by the candidate, under my supervision. The work presented here or any part of it has not been included in any other thesis submitted previously for the award of any degree or diploma from any other University or institution.



(Signature)

Dr. Thomas Pucadyil

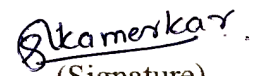
Associate Professor

IISER Pune

24/02/2019

## Declaration

I declare that this written submission represents my ideas in my own words and where others ideas have been included, I have adequately cited and referenced the original sources. I also declare that I have adhered to all principles of academic honesty and integrity and have not misrepresented or fabricated or falsified any idea/data/fact/source in my submission. I understand that violation of the above will be cause for disciplinary action by the Institute and can also evoke penal action from the sources that have thus not been properly cited or from whom proper permission has not been taken when needed.

  
(Signature)

Sukrut C Kamerkar  
Integrated PhD, IISER Pune  
Roll No. 20122020  
24/02/2019

## Acknowledgement

I want to express my gratitude to my supervisor, Dr. Thomas Pucadyil for his constant encouragement and support throughout my graduate studies. I would like to appreciate his patience, expertise and vast knowledge about all the subjects, which facilitated the completion of this work. His guidance helped me in evolving better research skills as well as in developing better communication abilities. Apart from the great supporter he also played a role of an excellent critique, which only propelled the work to be better. I would like to thank all the Pucadyil lab members for their suggestions on the work and assistance in editing the thesis. I would like to thank Prof. Mike Ryan and Felix Kraus from Monash University for the wonderful collaboration.

I would like to thank IISER Pune for their research facilities and excellent support staff.

“It’s the journey, not the destination that matters” this famous quote by T.S Eliot is indeed true, there are many friends who have enriched my Ph.D. journey in a very unique way. Firstly, I would like to thank my friends, Swapnil Pradhan and Sagar Varankar, for advising me to fill the application for the integrated Ph.D. program at IISER Pune. I have been fortunate to receive training under experienced graduate students at IISER- Sneha Bhogale, Chaitanya Mungi, and Sachin Holkar who were integral in inculcating scientific temperament. I would like to thank my friends Shrinivas Gharote, Jijith M. and Mukul Rawat for sharing everyday life and for many thoughtful discussions. I am truly grateful to my friends Rahi Reja, Chetan Vishwakarma, Ankitha Shetty, Ashish Surana, Neha Khetan, Aditi Madhuskar, Dnyanesh Dubal, Neeladri Sen, Sandip George, Anish Rao, Ron Sunny, Swati Sharma, Kashyap G., Jay Mangaonkar, Bharat Tandon, Abhishek Swarnakar, Ravi Devani and Mahesh Chand for their support which enabled me to stay focused and patient during hard times.

I have enjoyed working and learning with Vinayak Sadasivam, Pratima Singh, Gokul V.P, Pavithra Mahadevan, Krishnendu Roy, Soumya Bhattacharya, and Somya Madan.

I would like to thank CSIR for the graduate fellowship and DST-SERB for the generous travel award that enabled me to present my work internationally.

Special thanks to Devika Andhare, without her assistance and support I couldn't have imagined completing my Ph.D. Her motivations always brought out the best in me, for which I am grateful. I will always cherish countless discussions with her about science as well as about life in general.

Last but not the least I would like to thank my parents Chhaya and Chandrashekhar Kamerkar; and my sister Manali for their constant faith in me that allowed me to pursue my dreams.

Above all, I owe it all to God for granting me the health, wisdom, and strength that enabled completion of this work.

## Synopsis

Mitochondria are double-membrane organelles in eukaryotes, whose primary function is energy production through oxidative phosphorylation. Mitochondria have a diverse morphology, which is maintained by the cycles of division and fusion. As mitochondria cannot be synthesized *de novo*, they rely on fission for successful organelle-inheritance. Moreover, mitochondrial division is also essential for the maintenance of the cellular homeostasis, during cell death and is used as a tool to segregate damaged mitochondria. Dynamin-related protein 1 (Drp1), a member of the dynamin superfamily of proteins, is a crucial player involved in the mitochondrial division process. In the absence of Drp1, mitochondria show an elongated phenotype, which is reminiscent of a defective division process. Apart from its role in the mitochondrial division, Drp1 is also shown to be involved in the division of peroxisomes.

The domain architecture of Drp1 is similar to that of classical dynamins, which consists of a GTPase domain at the N-terminus, bundle signaling element and the stalk domain. However, instead of the lipid-binding pleckstrin homology domain found in classical dynamins, Drp1 has a variable, unstructured 100 amino acid loop called the B-insert, which is involved in binding to the mitochondrial lipid cardiolipin. Drp1 self-assembles into helical scaffolds and utilizes energy-derived from GTP-hydrolysis to remodel GUVs and liposomes to tubular intermediates. Current literature indicates that Drp1 is involved in membrane remodeling to facilitate fission but its direct involvement in the fission process remains debated.

Drp1 is predominantly cytosolic and relies on mitochondrial adaptor proteins (Mff, MiD49, and MiD51) for its recruitment to the mitochondria. Studies demonstrate that these adaptor proteins can act independently to recruit Drp1. However, their contribution, beyond recruiting Drp1 to mitochondrial and to the division process in general remains unknown. Recent reports suggest the involvement of the endoplasmic reticulum (ER) in causing mitochondrial constriction prior to Drp1-recruitment thus marking the site of mitochondrial division. A study by Voeltz and colleagues revealed the involvement of the classical dynamin-2 (Dnm2) in the mitochondrial division. Depletion of Dnm2 also led to significant mitochondrial elongation, with Drp1 remaining accumulated on constricted mitochondria. Thus, the

current model proposes cooperation between mitochondrial and classical dynamins, and that neither alone is sufficient for the mitochondrial fission. However, recent reports have questioned this model as mitochondrial fission occurs even in the absence of Dnm2, thus necessitating a re-evaluation of the contribution of each of these proteins to the mitochondrial division.

This thesis utilizes a bottom-up approach of reconstitution of the mitochondrial fission process and aims to understand the intrinsic functions of individual components, with a focus on Drp1's involvement in mitochondrial fission.

**Chapter 1** of the thesis gives an introduction to proteins involved in the regulation of mitochondrial division, briefly summarizing the known components involved in the fission machinery.

**Chapter 2** introduces the Supported Membrane Templates (SMrT), where the membrane is organized as a planar sheet and curved tubes resting on a passivated glass coverslips covalently modified with polyethylene glycol (PEG). These membrane topologies displayed on SMrTs mimic a non-constricted and constricted states of the mitochondria. This facile and robust assay system allows the use of various membrane lipid compositions and screens for protein function on a membrane surface displaying a range of curvatures. The mitochondrial-specific lipid cardiolipin can also be incorporated into SMrTs to closely mimic mitochondria.

In **Chapter 3**, using the SMrTs, I describe results indicating that Drp1 is sufficient to catalyze membrane fission. Fission is robust, with Drp1 capable of severing tubes as wide as 250 nm in radius. Although dynamin-2 can catalyze fission, it appeared to be severely restricted in its ability to sever wide tubes. Drp1 preferentially binds tubes over the supported lipid bilayer. This preference can be mapped to the B-insert region of Drp1. Stage-specific reconstitution reveals that unlike classical dynamins, which constrict membrane tubes in the absence of GTP, Drp1 requires GTP binding for membrane constriction. Drp1 requires GTP hydrolysis for causing further constriction of the membrane tube finally leading to fission. Together, our results indicate Drp1 to be self-sufficient in membrane fission and prompt a reevaluation of its involvement in the mitochondrial fission pathway.

Various adaptor proteins on the outer mitochondrial membrane govern Drp1 recruitment to the mitochondria. In **Chapter 4** effects of different adaptor proteins on Drp1-catalyzed membrane fission are probed using SMrTs. The presence of adaptor proteins Mff, MiD49, and MiD51 independently enhance Drp1 recruitment and fission. We also report a novel tendency of Mff to self-oligomerize and remodel membrane tubes, which in turn could determine the site of fission on mitochondria and peroxisomes. The effect of Mff on Drp1's binding and fission activity is systematically studied by varying cardiolipin concentration.

**Chapter 5** discusses functional differences among Drp1 Isoforms. Surprisingly, Drp1's longest Isoform (Isoform 1) is found to be impaired in membrane binding and fission, which is altogether different in behavior compared to Isoform 2 and Isoform 3. Since the various Isoforms are expressed in a tissue-specific manner, these results indicate a contribution from cell physiology to the evolution and selection of specific Isoforms of Drp1 that are different in their biochemical attributes.



# Table of Contents

|  |    |
|--|----|
| <b>Acknowledgement</b> .....   | 4  |
| <b>Synopsis</b> .....  | 6  |
| <b>Table of Contents</b> .....   | 9  |
| <b>Table of Figures</b> .....  | 12 |
| <b>Abbreviation</b> .....  | 13 |
| <b>1. Introduction</b> .....   | 15 |
| 1.1 <i>Dynamamin-related protein1 (Drp1)</i> .....   | 17 |
| 1.2 <i>Drp1-adaptor proteins</i> .....   | 18 |
| 1.3 <i>Role of ER tubule, actin and septins in mitochondrial fission machinery</i> .....                   | 19 |
| 1.4 <i>Dynamamin-2 mediated final fission step</i> .....   | 20 |
| <b>2. Supported Membrane Templates (SMrT): An assay to mimic diverse mitochondrial morphology</b> .....    | 22 |
| 2.1 Introduction.....  | 23 |
| 2.2 Materials and Methods .....  | 23 |
| 2.2.1 <i>Supported Membrane Templates (SMrT)</i> .....   | 23 |
| 2.4.2 <i>Tube radius estimation</i> .....  | 24 |
| 2.4.3 <i>Cardiolipin distribution</i> .....  | 24 |
| 2.4.4 <i>Fluorescence Microscopy</i> .....   | 25 |
| 2.4.5 <i>Fluorescence recovery after photobleaching analysis</i> .....                                     | 25 |
| 2.4.6 <i>RI8 dye tracing experiment</i> .....  | 25 |
| 2.4.7 <i>Image and statistical analysis, reproducibility</i> .....   | 25 |
| 2.3 Results.....   | 26 |
| 2.2.1 <i>Supported Membrane Templates (SMrT): An assay to mimic diverse mitochondrial morphology</i> ..... | 26 |
| 2.2.2 <i>Characterizations of SMrT</i> .....   | 28 |
| 2.4 Discussion.....  | 29 |
| <b>3. Drp1-catalyzed membrane fission</b> .....  | 31 |
| 3.1 Introduction.....  | 32 |
| 3.2 Methods and Material .....   | 32 |

|  |           |
|--|-----------|
| 3.2.1 Cloning, expression, purification and fluorescent labeling of proteins.....        | 32        |
| 3.2.2 GTPase Assay.....  | 34        |
| 3.2.3 Supported Membrane Templates (SMrT).....   | 34        |
| 3.2.4 Image and statistical analysis, reproducibility.....                               | 34        |
| 3.3 Results .....  | 35        |
| 3.3.1 Biochemical characterization of Drp1.....  | 35        |
| 3.3.2 Drp1 membrane binding and self-assembly.....                                       | 36        |
| 3.3.3 B-insert: Membrane binding site on Drp1.....                                       | 38        |
| 3.3.4 Drp1-catalyzed membrane fission.....   | 39        |
| 3.3.5 Mechanism of Drp1-catalyzed membrane fission.....                                  | 41        |
| 3.4 Discussion.....  | 44        |
| <b>4. Role of mitochondrial adaptor proteins in Drp1-catalyzed membrane fission.....</b> | <b>46</b> |
| 4.1 Introduction.....  | 47        |
| 4.2 Materials and Methods.....   | 47        |
| 4.2.1 Cloning, expression and purification of proteins.....                              | 47        |
| 4.2.2 Labeling of Mff with extrinsic fluorophores.....                                   | 48        |
| 4.2.3 Supported Membrane Templates (SMrT).....   | 48        |
| 4.2.4 mEGFP encapsulated Supported Membrane Templates.....                               | 48        |
| 4.3 Results.....   | 49        |
| 4.3.1 Adaptor proteins facilitate Drp1-catalyzed membrane fission.....                   | 49        |
| 4.3.2 Organization of Mff on membrane.....   | 51        |
| 4.3.3 Coiled-coil domain involved in Mff oligomerization.....                            | 53        |
| 4.3.4 Mff facilitates Drp1 recruitment to membrane.....                                  | 54        |
| 4.3 Discussion.....  | 56        |
| <b>5. Functional differences in Drp1 Isoform.....</b>                                    | <b>57</b> |
| 5.1 Introduction.....  | 58        |
| 5.2 Materials and Methods.....   | 58        |
| 5.2.1 Cloning, expression and purification of proteins.....                              | 58        |
| 5.2.2 Supported Membrane Templates (SMrT).....   | 58        |
| 5.2.3 GTPase assay.....  | 59        |
| 5.3 Results.....   | 59        |

|  |           |
|--|-----------|
| 5.3.1 <i>Drp1 Isoform 1 is defective in membrane recruitment and fission on Mff coated tubes</i> .....                         | 59        |
| 5.3.2 <i>Isoform 1 is defective in fission of CL-containing tubes</i> .....  | 62        |
| 5.3.3 <i>Isoform 1 is defective in binding cardiolipin-containing membranes despite possessing a functional B-insert</i> ..... | 64        |
| 5.4 Discussion.....  | 65        |
| <b>6. Summary</b> .....  | <b>67</b> |
| <b>Manuscripts published</b> .....   | <b>69</b> |
| <b>References</b> .....  | <b>70</b> |

## Table of Figures

|  |    |
|--|----|
| Figure 1.1 Domain architecture of Dynamin-related protein1.....  | 18 |
| Figure 1.2 Model for mitochondrial fission.....  | 20 |
| Figure 2.1 Schematic for preparation of <u>S</u> upported <u>M</u> embrane <u>T</u> emplates<br>(SMrT).....                    | 26 |
| Figure 2.2 <i>Supported Membrane Templates (SMrT)</i> : An assay to mimic diverse<br>mitochondrial morphology.....             | 27 |
| Figure 2.3 Workflow for tube size estimation.....  | 28 |
| Figure 2.4 Characterizations of Supported Membrane Templates.....  | 29 |
| Figure 3.1 Biochemical characterization of Drp1.....   | 35 |
| Figure 3.2 Self-assembly of Drp1 on the membrane tubes.....  | 37 |
| Figure 3.3 Design of minimal B-insert construct.....   | 38 |
| Figure 3.4 B-insert: membrane recruitment site in Drp1.....  | 39 |
| Figure 3.5 Drp1-catalyzed membrane fission.....  | 41 |
| Figure 3.6 Mechanism of Drp1-catalyzed membrane fission.....   | 43 |
| Figure 4.1 Schematic of Mff, MiD49/51 and their mimics used in Supported<br>Membrane Templates.....                            | 49 |
| Figure 4.2 Adaptor proteins facilitate Drp1-catalyzed membrane fission.....  | 50 |
| Figure 4.3 Organization of Mitochondrial fission factor on membrane.....   | 52 |
| Figure 4.4 Schematic of Mff with deletion of the coiled-coil and transmembrane<br>domain.....                                  | 53 |
| Figure 4.5 Coiled-coil region involved in oligomerization and membrane<br>constriction activity of Mff.....                    | 53 |
| Figure 4.6 Mff mediated Drp1 recruitment to membrane tubes and fission.....  | 55 |
| Figure 5.1 Schematic comparing Drp1 Isoforms.....  | 60 |
| Figure 5.2 Drp1 Isoform 1 is defective in membrane recruitment and fission on<br>Mff coated supported membrane templates.....  | 62 |
| Figure 5.3 Isoform 1 is defective in fission of CL-containing tubes.....   | 63 |
| Figure 5.4 Isoform 1 is defective in binding cardiolipin-containing membranes<br>despite possessing a functional B-insert..... | 65 |

## Abbreviations

|            |   |
|------------|---|
| 6xHis      | 6xHistidine tag   |
| apo state  | no nucleotide bound state   |
| Ax647-SA   | Alexa Fluor™ 647 conjugated streptavidin (Invitrogen)   |
| Ax488-Drp1 | Alexa Fluor™ 488 C5 maleimide labeled Dynamin related protein 1   |
| Ax488-Mff  | Alexa Fluor™ 488 C5 maleimide labeled Mitochondrial fission factor  |
| Caf4       | CCR4-associated factor 4  |
| CL         | Cadiolipin  |
| DGS-NiNTA  | 1,2-dioleoyl-sn-glycero-3-[(N-(5-amino-1-carboxypentyl)-iminodiacetic acid) succinyl] (nickel salt)                       |
| DiD        | 1,1'-dioctadecyl-3,3',3'-tetramethylindodicarbocyanine, 4-chlorobenzenesulfonate salt ('DiD' solid)                       |
| Dnm2       | Dynamin2  |
| DOPC       | 1,2-dioleoyl-sn-glycero-3-phosphocholine  |
| DOPS       | 1,2-dioleoyl-sn-glycero-3-phospho-L-serine (sodium salt)  |
| Drp1       | Dynamin related protein 1   |
| Drp1-mEGFP | Dynamin related protein 1 fused to monomeric Enhanced Green Fluorescent Protein at C terminus                             |
| Drp1± GFP  | Equimolar mixture of Dynamin related protein 1-monomeric Enhanced Green Fluorescent Protein and Dynamin related protein 1 |
| EDTA       | Ethylenediaminetetraacetic acid   |
| Fis1       | Mitochondrial fission 1 protein   |
| GDP        | Guanosine-5'-diphosphate, Sodium salt   |
| GMP-PNP    | Guanosine-5'-[(β,γ)-imido]triphosphate, Trisodium salt  |
| GTP        | Guanosine 5'-triphosphate, Sodium salt  |
| GUV        | Giant Unilamellar Vesicle   |
| HBS        | Buffer consisting of 20mM HEPES, 150mM NaCl pH7.4   |
| HKS        | Buffer consisting of 20mM HEPES, 150mM KCl pH7.4  |
| Iso        | Isoform   |
| kDa        | kilo Dalton   |
| Mdv        | Mitochondrial division protein 1  |

|                      |  |
|----------------------|--|
| mEGFP                | monomeric Enhanced Green Fluorescent Protein   |
| mEGFP-Drp1           | monomeric Enhanced Green Fluorescent Protein fused to Drp1 at N-terminus                                     |
| Mff                  | Mitochondrial fission factor   |
| MgCl <sub>2</sub>    | Magnesium Chloride   |
| MiD49                | Mitochondrial dynamics protein 49kDa   |
| MiD51                | Mitochondrial dynamics protein 51kDa   |
| mins                 | minutes  |
| mt-DNA               | Mitochondrial Deoxy Nucleic Acid   |
| N                    | Number of experimental repeats   |
| NAO                  | Nonyl acridine orange  |
| NiCl <sub>2</sub>    | Nickel(II) chloride  |
| nm                   | nano meter   |
| n <sub>SLB</sub>     | Number of Supported Lipid Bilayer analyzed   |
| N <sub>SMrT</sub>    | Number of independent SMrT template assay performed  |
| n <sub>tube</sub>    | Number of Supported Lipid Bilayer analyzed   |
| <i>p</i> -TxRed DHPE | <i>para</i> -Texas Red® 1,2-Dihexadecanoyl- <i>sn</i> -Glycerol-3-phosphoethanolamine, Triethylammonium Salt |
| RhPE                 | 1,2-dioleoyl- <i>sn</i> -glycerol-3-phosphoethanolamine-N-(lissamine rhodamine B sulfonyl) (ammonium salt)   |
| ROI                  | Region of interest   |
| s                    | second   |
| S.D                  | Standard Deviation   |
| sec                  | second   |
| SLBs                 | Supported Lipid Bilayer  |
| SMrT                 | Supported Membrane Templates   |
| StrepII              | Streptactin tag  |
| VPEK                 | Valine-Proline-Glutamic acid-Lysine amino acid sequence  |
| VPER                 | Valine-Proline-Glutamic acid-Arginine amino acid sequence  |
| μm                   | micrometer   |

# **Chapter 1**

## **Introduction**

## 1. Introduction

Mitochondria are ubiquitous double-membrane organelles present in eukaryotic cells, whose primary function is the production of cellular ATP<sup>1</sup>. They are thought to have originated from engulfment of an aerobic bacterium by a larger archaeobacterium, consequently leading to a close endosymbiotic relationship in the time course of evolution<sup>2</sup>. The morphology and number of mitochondria vary across different tissues and is maintained by continuous cycles of fission and fusion<sup>1</sup>. Fusion acts as a mode of complementation of partially damaged mitochondria by mixing the mitochondrial contents and mitochondrial DNA. Mitochondrial fission is required for the faithful inheritance of mitochondria from parent to the daughter cells, as it cannot be synthesized *de novo*<sup>3</sup>. Mitochondrial fission is also required in mitochondrial quality control by facilitating the removal of damaged mitochondria<sup>4</sup> and apoptosis during high cellular stress<sup>5</sup>. Various diseases have been implicated due to mutations in the proteins involved in mitochondrial fusion and fission pathway<sup>6,7</sup>. A plethora of molecules are involved in mitochondrial fission and fusion, key regulators being large GTPases of the dynamin superfamily<sup>8</sup>.

### Mitochondrial division machinery

A proper balance between mitochondrial fission and fusion maintains mitochondrial morphology, dynamics and ensures cellular homeostasis. Cellular and genetic studies have identified majorly two classes of molecules involved in mitochondrial fission. First is the dynamin-related protein1 (Drp1)<sup>9,10</sup> which is a crucial player in mitochondrial fission. Like dynamin, Drp1 is thought to oligomerize and physically constrict mitochondria and catalyze fission. However, most of the Drp1 is cytosolic thus necessitating a specialized recruitment apparatus to effectively catalyze fission. The second class of molecules is Drp1-adaptor proteins; fission protein1 (Fis1), mitochondrial fission factor (Mff) and mitochondrial division proteins of 49 and 51 kDa (MiD49/51), which recruit Drp1 to the mitochondrial surface. Apart from these, imaging studies suggest endoplasmic reticulum marks the site of constriction on mitochondrial prior to the Drp1 recruitment<sup>11</sup>. Many proteins including cytoskeletal proteins are involved in regulating ER-mitochondrial contact sites<sup>12</sup>. Recently, dynamin-2 has been implicated in mediating the final scission step



during the mitochondrial fission<sup>13</sup>. EM studies indicate that the mitochondrial inner membrane can divide without necessitating outer mitochondrial membrane fission<sup>14</sup>, however how inner membrane undergoes fission is still unknown.

### **1.1 Dynamin-related protein1 (Drp1)**

Dynamin-related protein1 (Drp1) is a crucial player involved in the mitochondrial fission. Drp1 knockout or expression of dominant negative mutant leads to an elongated hyper-fused mitochondrial morphology<sup>9,10,15,16</sup>. Drp1 null mice die after embryonic day 11.5 due to neuronal developmental defects<sup>15,16</sup>. Drp1 has also been suggested to be involved in mediating peroxisomal fission<sup>17</sup>, a single membrane organelle involved in the metabolism of long-chain fatty acids<sup>18</sup>. Drp1 consists of a GTPase domain involved in GTP hydrolysis at the N-terminus followed by bundle signaling element (BSE) which relays conformational changes from G to the stalk domain, stalk domain which is involved in Drp1 multimerization<sup>19</sup> and binding to the mitochondrial adaptor proteins<sup>20</sup> and the B-insert which is the putative membrane-binding region<sup>21</sup> (Figure 1.1A, crystal structure of Drp1 with the respective domains is represented in Figure 1.1B). Drp1 has been shown to assemble in higher order structures with the non-hydrolysable analog of GTP<sup>22,23</sup> and ring like intermediates with ~10nm radius with GTP<sup>23,24</sup>. Drp1 is also able to tubulate liposomes and giant unilamellar vesicles (GUVs)<sup>19,21,25-27</sup>. These observations suggest that the most Drp1 seems to be capable of is constricting the underlying membrane but not catalyzing fission.

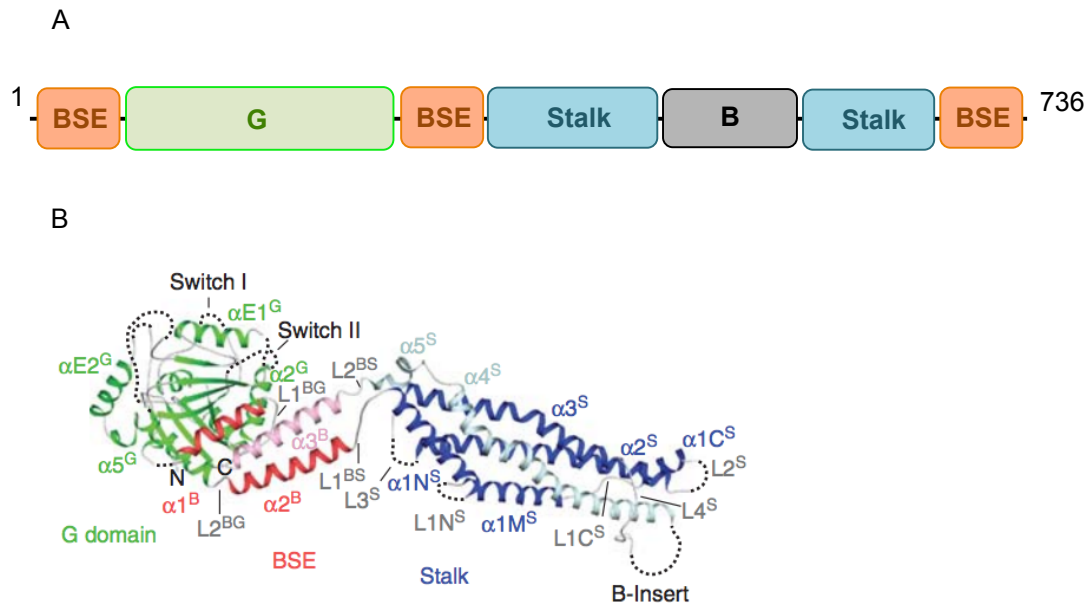


**Figure 1.1 Domain architecture of Dynamin-related protein1**

(A) Schematic showing the domain architecture of Drp1 based on its structure, G stands for the GTPase domain, BSE stands for bundle signaling element, B stands for the B-insert. (B) Crystal structure of Drp1 showing G domain in green, bundle signaling element in red and stalk domain in blue. The B-insert is denoted by a dotted line. (The image is reproduced from Fröhlich *et al.* Structural insights into oligomerization and mitochondrial remodeling of dynamin 1-like protein. *EMBO J.* **32**, 1280–92, 2013).

## 1.2 Drp1-adaptor proteins

The second sets of proteins that are implicated in the mitochondrial division are adaptors involved in the recruitment of Drp1 from cytosol to mitochondrial outer membrane. These are transmembrane domain-containing proteins that are present on the outer mitochondrial membrane. Fis1, Mdv1, Caf4 are adaptors in yeast while Mff and MiD49/51 are involved in the mammalian mitochondrial division<sup>28</sup>. Fis1 was one of the first Drp1 adaptors identified in budding yeast. In yeast, the absence of Fis1 leads to an elongated mitochondrial morphology, similar to that of Drp1 knockdown<sup>29</sup>. However, it was later found that mammalian homolog of Fis1 does not play a crucial role in mitochondrial fission<sup>30</sup>, instead it is involved in mitophagy<sup>31</sup>. Similarly, mammals do not have a homolog of Mdv1 and Caf4, two other yeast adaptor proteins that recruit Drp1. In mammals, the function of Drp1 recruitment is attributed to Mff, MiD49 and MiD51<sup>6</sup>.

## **Mff**

Mff (Mitochondrial fission factor), a tail-anchored protein in the outer mitochondrial membrane, was identified as a factor affecting the mitochondrial morphology in a genetic screen using siRNA in *drosophila* S2 cells<sup>32</sup>. The knockdown of Mff leads to an elongated mitochondrial morphology, which is similar to Drp1 knockdown. Mff overexpression leads to fragmented mitochondrial morphology<sup>30</sup>, indicating that Mff is a crucial player involved in Drp1 recruitment from cytosol to mitochondria. Immunoprecipitation experiments suggest that Mff and Drp1 physically interact with each other<sup>30</sup>. Mff gets recruited to the site on constriction independent of Drp1<sup>33</sup>. Together, these results indicate that Mff is involved in Drp1 recruitment to the mitochondrial surface and defining the site of fission. Interestingly, Mff is also present on the peroxisomal membrane and its knockdown affects peroxisomal morphology as well, suggesting core division machinery is shared between mitochondria and peroxisomes<sup>32,34</sup>.

## **MiD49/MiD51**

MiD49 (Mitochondrial dynamics protein 49 kDa, MIEF2) and MiD51 (Mitochondrial dynamics protein 51 kDa, MIEF1) are closely related proteins present on the outer mitochondrial membrane. Both the proteins have a transmembrane domain at the N-terminus thus displaying bulk of the protein into the cytosol. Knockdown of both the MiD proteins lead to an elongated mitochondrial morphology<sup>35</sup>. Using yeast two-hybrid assays and coimmunoprecipitation it has been shown that MiD proteins and Drp1 directly interact with each other<sup>35</sup>. However, unlike Mff, overexpression of MiD's leads to elongated mitochondrial phenotype<sup>36</sup>. Thus exact roles of MiD proteins in mitochondrial fission is still speculated.

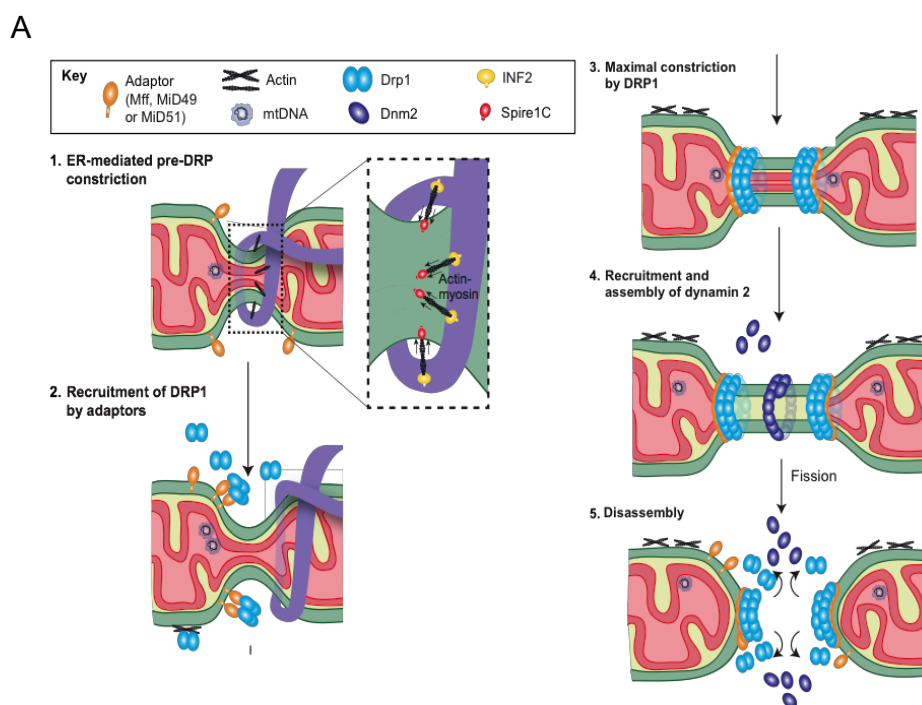
### **1.3 Role of ER tubule, actin and septins in mitochondrial fission machinery**

Although ER-mitochondrial contact sites were described in 1960<sup>37</sup>, it was only recently that they were implicated in the mitochondrial fission. ER contact sites on mitochondria marked about 94% of fission events wherein ER tubules wrap around mitochondria, leading to a constriction and thus facilitating fission<sup>33</sup>. Drp1 adaptor proteins Mff, MiD49/51 were observed to be localized at such pre-constricted mitochondrial state, thus marking the site for subsequent Drp1 recruitment and

mitochondrial fission<sup>38</sup>. Recently, inverted formin on ER<sup>39</sup> and spire 1C<sup>40</sup> on mitochondria were observed to polymerize actin. Following which myosin II in conjunction with them was shown to promote mitochondrial constriction<sup>41</sup>. Independent study also revealed Arp2/3 mediating actin polymerization on the mitochondria and promoting its constriction<sup>42</sup>. Similar to actin, septins were implicated in the mitochondrial division process. Septins were shown to directly interact with Drp1, promoting its recruitment to mitochondria. Depletion of septins 2/7 led to an elongated mitochondrial morphology<sup>43</sup>. Taken together all these reports suggest that mitochondrial fission is orchestrated and tightly regulated by a large number of proteins in the cytoplasm.

#### 1.4 Dynamin-2 mediated final fission step

In addition to all these studies, a recent study by Lee *et al.* implicated dynamin-2 to be involved in the mitochondrial fission. Depletion of dynamin-2 by siRNA led to an elongated mitochondrial morphology similar to the Drp1 knockdown<sup>13</sup>. According to this model, dynamin-2 assembles on Drp1 constricted mitochondria and leads to final mitochondrial fission (Figure 1.2).



Based on Lee et al. (2016) Nature  
Kraus and Ryan (2017) J. Cell Sci.

## Figure 1.2 Model for mitochondrial fission

(A) Step1 ER tubule marks site for mitochondrial constriction. ER physically wraps around mitochondria, inverted formin on ER and spire2C on mitochondria promote mitochondrial constriction. Step2 Drp1 adaptor proteins cluster at the site of constriction leading to Drp1 requirement. Step3 Drp1 constricts mitochondria; step4 dynamin2 assembles and catalyzes final fission and disassembles in step5. (The image is reproduced from Kraus, F. & Ryan, M. T. The constriction and scission machineries involved in mitochondrial fission. *J. Cell Sci.* **130**, 2953–2960, 2017).

The current model proposes cooperation between the mitochondrial and classical dynamins, and that neither alone is sufficient for mitochondrial fission (Figure 1.2).

However, recent reports have questioned this model as mitochondrial and peroxisomal fission occurs even in the absence of dynamin-2<sup>44,45</sup>. Whether Drp1 is sufficient to catalyze membrane fission remains an open question.

## **Chapter 2**

### **Supported Membrane Templates (SMrT): An assay to mimic the diverse mitochondrial morphologies**

## 2.1 Introduction

Mitochondria have a diverse morphology across cell types<sup>46</sup>; their morphology varies in response to the cellular environment<sup>47</sup> and during mitotic division<sup>48</sup>. Their movement, size and shape are maintained by cytoskeletal elements and balanced cycles of fusion and fission<sup>49</sup>. These mitochondrial dynamics are essential for quality control and inheritance<sup>50</sup>. Defects in the fission and fusion cycle have been linked to various neurodegenerative disorders such as Parkinson's, Alzheimer's and Huntington's disease<sup>51</sup>. Just prior to the fission, mitochondria undergo a dramatic remodeling step, which is mediated by a plethora of molecules<sup>12</sup>. Drp1 is one of the critical molecules involved in the mitochondrial division, its absence leads to a hyper-fused mitochondrial morphology<sup>52</sup>. Various assay system such as Giant Unilamellar Vesicles (GUVs)<sup>25</sup> and liposomes<sup>21,26</sup> have demonstrated Drp1's role in membrane remodeling but whether it is sufficient to catalyze fission is still unclear. These assays, however, have their limitation due to the planar nature of the GUVs and end point-based readouts.

In order to circumvent these issues, we have devised Supported Membrane Templates (SMrT), which comprises of an array of narrow tubes pinned on a passivated glass surface, and planar Supported Lipid Bilayers (SLB)<sup>53</sup>. These tubes have variable dimensions which mimic the constricted mitochondrial morphology<sup>11,54</sup>, while the SLB mimics the non-constricted mitochondrial morphology. This assay system can thus be used to monitor various membrane curvature dependent processes. Besides being robust and facile assay, it also has a unique advantage of detecting membrane remodeling and fission reaction in real-time. The SMrTs can be made with various kinds of lipids, which allows a unique handle in mimicking different organellar membranes.

## 2.2 Materials and Methods

### 2.2.1 Supported Membrane Templates (SMrT)

A mixture of DOPC, cardiolipin (Avanti Polar Lipids) and *p*-Texas red DHPE (74:25:1 mol%) was aliquoted in a glass vial to make the final concentration of 1mM

in chloroform. *p*-Texas red DHPE was separated from mixed isomer Texas red DHPE (Invitrogen) using thin-layer chromatography on silica gel plate (Sigma) as described elsewhere<sup>55</sup>. Lipid stocks were stored at -40°C and brought to room temperature before use. SMrTs were prepared as mentioned in<sup>53</sup>. Briefly, 2-3µl (1 nmol of total lipid) of chloroform-dissolved stock was spread on PEGylated coverslip, dried and assembled in the flow cell (FCS2, Bipotechs, PA). Lipids were hydrated in buffer containing 20 mM HEPES pH 7.4, 150 mM KCl leading to the formation of vesicles. These vesicles get extruded into membrane tubes when subjected to a shear flow of buffer (~30 mm s<sup>-1</sup> particle velocity inside the chamber). Membrane tubes get pinned to the surface due to micro defects present on the coverslip, which results in an array Supported Membrane Templates (SMrT) on a PEGylated surface.

### 2.2.2 Tube radius estimation

Tube size estimation was performed as described earlier<sup>53,56,57</sup>. Briefly, images of the Supported Lipid Bilayer (SLB) (formed where lipid was spotted) for each SMrT preparation were acquired, background corrected to estimate calibration constant (k1), which is defined as integrated fluorescence density (ID) per unit area (µm<sup>2</sup>). Integrated fluorescence density of a tube of length l (µm) was converted to tube radius (r) using equation  $r = ID(k1 * 2\pi * l)^{-1}$ . Maximum fluorescence intensity along the length of the tube was plotted against its radius (r) to get second calibration constant (k2). Maximum pixel intensity on the tube was divided by k2 to get the radius.

### 2.2.3 Cardiolipin distribution

To assess cardiolipin distribution on SLBs and tubes, supported membrane templates containing DOPC:CL:BiotinCapDOPE (74:25:1mol%) were prepared. 1µM of Alexa Fluor® 647 conjugated streptavidin (Invitrogen, Ax647-SA) was recruited on SLBs and tubes using biotinylated lipid and used as a membrane marker since streptavidin-biotin interaction is curvature independent<sup>58</sup>. 400 µM of Nonyl acridine orange (NAO, Thermo scientific) was flowed into the flow cell to detect the presence of cardiolipin<sup>59</sup>. The ratio of fluorescence intensity of NAO to Ax647-SA was compared across SLBs and tubes to calculate a relative distribution of cardiolipin.



#### **2.2.4 Fluorescence microscopy**

SMrT were imaged using Olympus IX71 inverted microscope equipped with a 100X, 1.4 NA oil-immersion objective. Fluorescent probes were excited with a stable LED light source (Thor Labs) and fluorescence emission was collected through filters (Semrock) with excitation/emission wavelength band passes of  $482 \pm 35$  nm/ $536 \pm 40$  nm for Alexa-488/GFP-tagged protein and  $562 \pm 40$  nm/ $624 \pm 40$  nm for Texas red probes simultaneously on two Evolve 512 EMCCD cameras (Photometrics). Image acquisition was controlled by Micro-Manager software (Molecular Devices).

#### **2.2.5 Fluorescence recovery after photobleaching analysis**

Fluorescence recovery after photobleaching was carried out on membrane tubes of SMrT containing 1 mol% of Rhodamine PE (RhPE, Avanti Polar Lipids) using 60x/1.4 NA oil-immersion objective on Zeiss LSM 710 laser scanning confocal microscope. Images were acquired at an optical zoom of 3.0 and argon laser power of 2% and 150 iterations at 100% transmission were used for photobleaching. Standardization of imaging parameters was performed to minimize photobleaching during acquisition.

#### **2.2.6 R18 dye tracing experiment**

1  $\mu$ M octadecyl rhodamine B (R18, Avanti Polar Lipids) (prepared in the assay buffer) was flown in SMrT with a lipid composition of DOPC: DOPS: DiD (69:40:1 mol%). Images were acquired in rhodamine channel at an interval of 100 milliseconds.

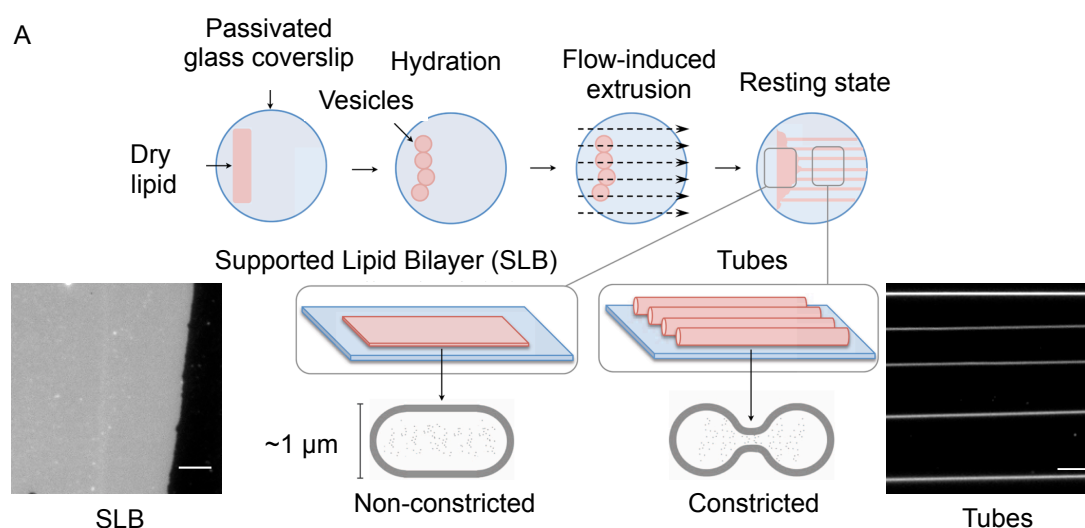
#### **2.2.7 Image and statistical analysis, reproducibility**

Image analysis was carried out using Fiji<sup>60</sup>. Statistical analysis was carried out using GraphPad Prism (version 5.0a).  $n_{\text{SLB}}$  or  $n_{\text{tube}}$  refers to the number of SLBs or tubes analyzed in a single SMrT preparation.  $N_{\text{SMrT}}$  refers to the number of independent supported membrane templates preparations.

## 2.3 Results

### 2.3.1 Supported Membrane Templates (SMrT): An assay to mimic diverse mitochondrial morphologies

Mitochondria are dynamic organelles present in eukaryotes, which undergo constant cycles of division and fusion. Unlike the oversimplified textbook image in which mitochondria are depicted to have a sausage-like structure floating in the cytosol, they have a complex morphology, which varies in accordance to the cellular requirements<sup>61,62</sup> as well as across different cell types<sup>46</sup>. Mitochondrial morphology also varies during its division<sup>48</sup>, ranging from a planar morphology in resting state to highly constricted morphology just prior to the fission<sup>11,54</sup>. The supported membrane templates (SMrT)<sup>53,63,64</sup> was used to mimic these various different mitochondrial morphologies. Protocol for making SMrT is described briefly in the materials and methods of this chapter (Also see Figure 2.1 A for schematic). The supported lipid bilayer present at the source mimics the non-constricted mitochondrial morphology while tubes mimic the constricted mitochondrial morphology just prior to fission (Figure 2.1 A, schematic).



**Figure 2.1 Schematic for preparation of Supported Membrane Templates (SMrT)**

(A) Schematic of SMrT system. Supported lipid bilayer (SLB) mimics non-constricted mitochondrial morphology while tubes mimic constricted mitochondrial morphology. Lipids are doped with 1 mol% *p*TxRed-DHPE to aid visualization Scale bar = 5 $\mu$ m (Schematic prepared by Thomas Pucadyil).

Fluorescent Recovery After Photobleaching (FRAP) of rhodamine PE-labeled membrane tube in the SMrT showed almost 100% recovery confirming that lipids are freely diffusible (Figure 2.2 A, B and C). In conjunction to FRAP, lipid diffusion was also assessed using the fusion of Octadecyl Rhodamine B Chloride (R18)<sup>65,66</sup> on SMrT. Upon fusion of R18 micelles to tubes, there was a burst of fluorescence, which spreads across the entire length of the tube (Figure 2.2 D) indicating that lipids are free to diffuse.

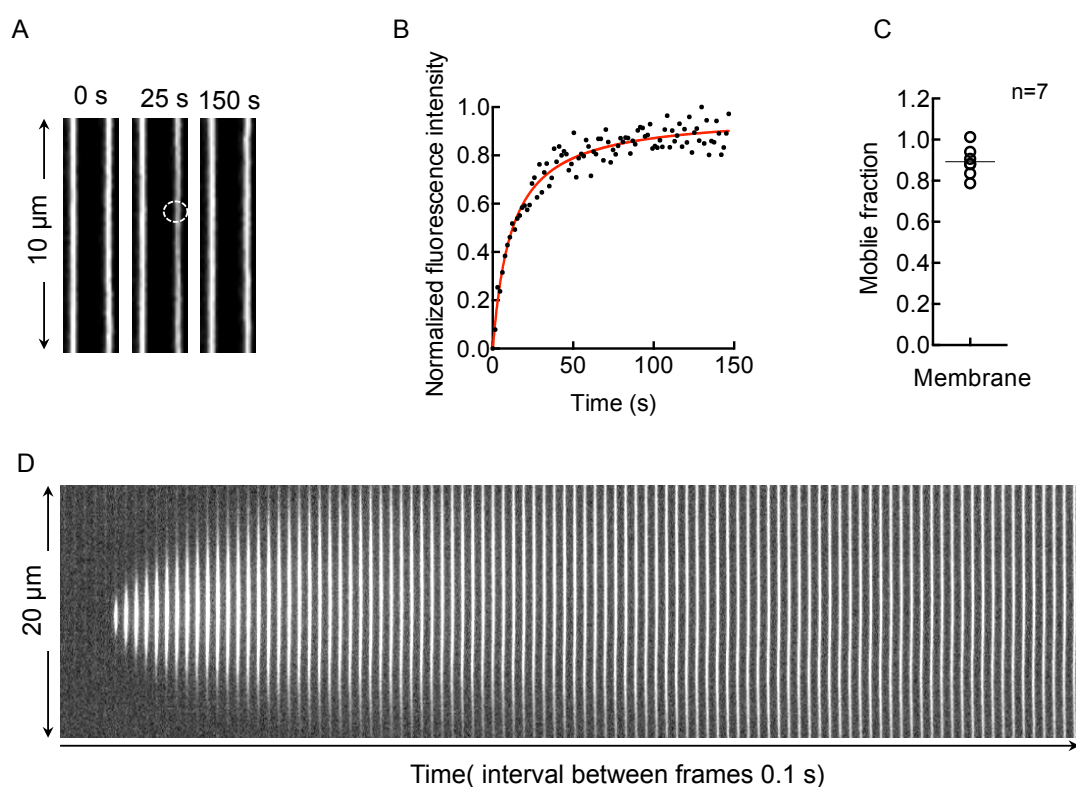


**Figure 2.2 Supported Membrane Templates (SMrT): An assay to mimic diverse mitochondrial morphologies**

(A) Fluorescent Recovery After Photobleaching (FRAP) of rhodamine PE-labeled membrane tube in SMrT. Images acquired during a FRAP experiment. The dotted circle marks the bleached region. (B) Fluorescence recovery data (black dots) after photobleaching a membrane tube, fitted to a one-dimensional recovery equation (red trace) and mobile fraction (C). (D) Stills from a movie depicting a single R18 fusion event, acquired while flowing in Octadecyl Rhodamine B Chloride (R18) on the SMrT.

### 2.3.2 Characterizations of Supported Membrane Templates

The tube sizes were estimated using a previously described protocol<sup>53,56,57</sup> (Also briefly described in materials and methods section, see Figure 2.3 A).

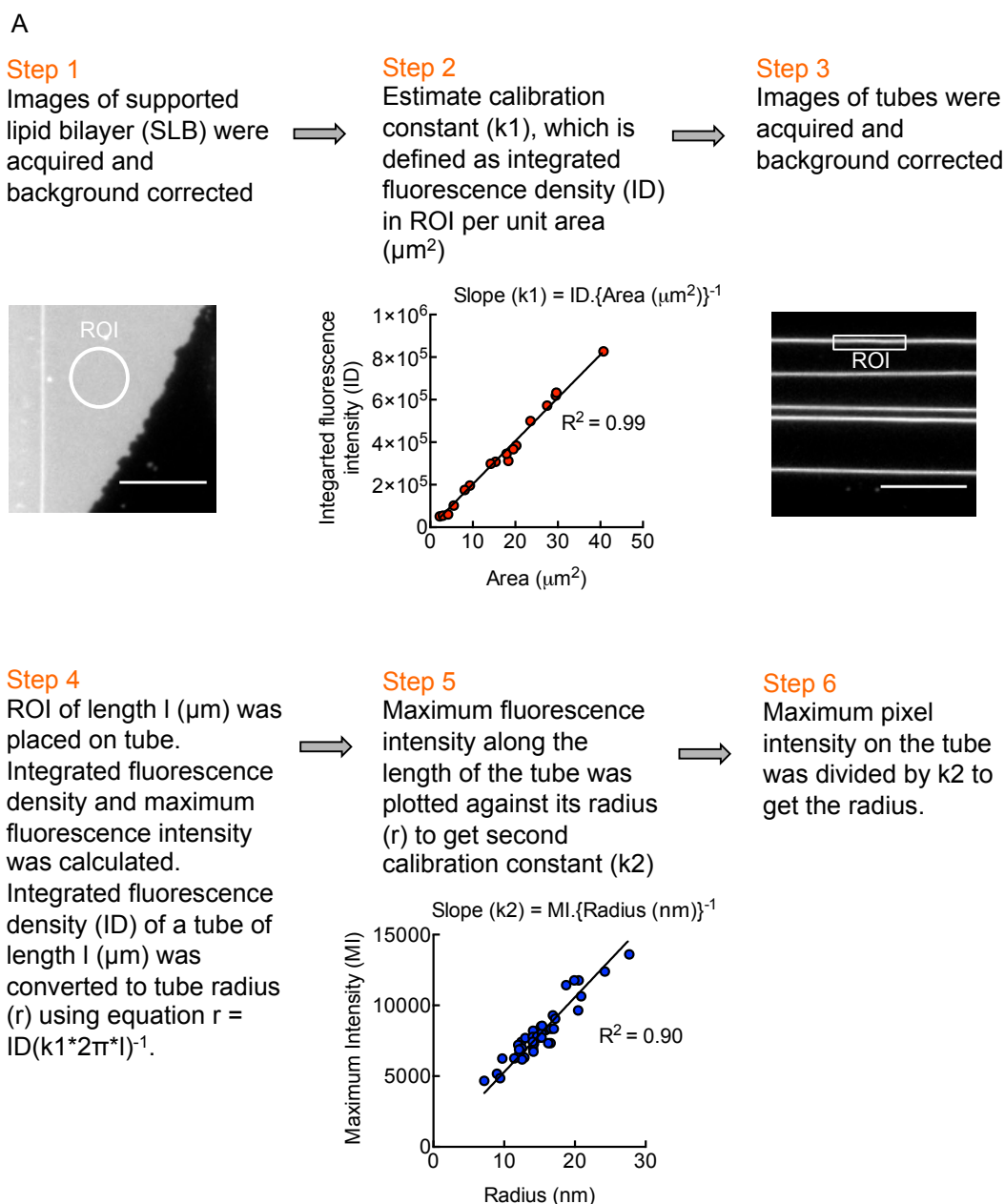


**Figure 2.3 Workflow for tube size estimation**

(A) Schematic describing the workflow for the tube size estimation. Scale bar = 10  $\mu\text{m}$ .

The tube size depends on the force applied to extrude tubes from the reservoir. These ranged from as small as 6 nm to as wide as 360nm in radius, median being at

21nm in radius (Figure 2.4 A). Thus, supported membrane templates have a unique benefit of sampling many different membrane topologies at the same time. Cardiolipin, dimeric lipid consisting of two phosphatidic acids connected by a glycerol backbone, is uniquely present in mitochondria and peroxisomes<sup>67</sup>. The outer mitochondrial membrane has 5 mol% whereas it is enriched to 25 mol% in the inner leaflet<sup>68</sup>. Thus, in order to mimic the mitochondrial membrane, cardiolipin was incorporated in the templates<sup>69</sup>. Using an anionic lipid sensor nonyl acridine orange (NAO)<sup>59</sup> and membrane curvature-insensitive Ax647-SA<sup>58</sup> recruited to the templates with biotinylated lipids revealed cardiolipin to be evenly distributed between the tubes and SLB (Figure 2.4 B, C).

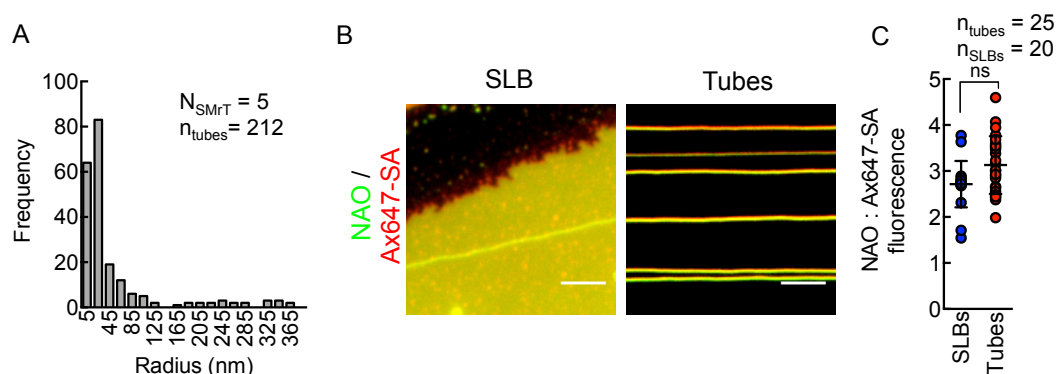


**Figure 2.4 Characterizations of Supported Membrane Templates**

(A) Histogram of the tube radius in SMrT experiment.  $N_{SMrT}$  indicates the number of SMrT system analyzed.  $n_{tubes}$  indicates the number of tubes analyzed. (B) Analyzing cardiolipin distribution on the tubes and SLB. Alexa-647 streptavidin was used as a membrane marker; Nonyl acridine orange (NAO, Thermo scientific) was flowed into the flow cell to detect the presence of cardiolipin. Scale bar = 5  $\mu$ m. (C) The ratio of fluorescence intensity of NAO to Alexa647 streptavidin (Ax647-SA) was compared across SLB and the tube to calculate the relative distribution of cardiolipin. The data represent mean  $\pm$  S.D; the number of tubes and SLBs analyzed is indicated by  $n_{tubes}$  and  $n_{SLBs}$  respectively. The significance was calculated using the Mann-Whitney test.

## 2.4 Discussion

The Supported Membrane Templates (SMrT) provide a high-throughput platform for screening proteins that can bind and remodel the membrane tubes, ranging from 10 nm to 400 nm, which would mimic the constricted mitochondrial

morphology prior to its division. The Supported Lipid Bilayer at the source enables probing of protein binding to the planar morphology of non-constricted mitochondria. Since the entire assembly is housed in a flow-cell, one can wash off unbound proteins using controlled flow. Even though membrane tubes are pinned on the passivated glass surface; lipids are free to diffuse as was seen by the FRAP analysis and R18 fusion assay.

Importantly, the supported membrane templates are amenable to inclusion of a variety of lipid compositions and can be used to mimic various organelles. Both mitochondria and peroxisomes are enriched in the lipid cardiolipin<sup>67,70</sup>. Although cardiolipin is predominantly found in the inner mitochondrial membrane as compared to the outer membrane<sup>68</sup>, just prior to mitochondrial fission it is predicted to be enriched at the contact sites between the inner and outer mitochondrial membrane<sup>71-73</sup>. Such localized cardiolipin microdomains are hypothesized to serve as a platform for Drp1 recruitment and subsequent mitochondrial division<sup>74</sup>. Indeed Drp1 seems to specifically recognize cardiolipin<sup>75,76</sup> and shows stimulated GTPase activity in the presence of cardiolipin containing liposomes<sup>25</sup>. Using NAO (probe for cardiolipin) and Alexa-647 conjugated streptavidin as a counter probe for membrane; cardiolipin was found to be uniformly distributed across the tubes and SLBs.

A mimic of mitochondria and peroxisome outer membrane made by inclusion of cardiolipin provides a template to study Drp1 function.

**Chapter 3**  
**Drp1-catalyzed membrane fission**

### 3.1 Introduction

Mitochondria, a dynamic double-membrane organelle in eukaryotes, undergo constant cycles of fission and fusion. Mitochondria rely on fission and growth cycles for its inheritance, since it cannot be synthesized *de novo*<sup>3</sup>. Mitochondrial division is also essential for its quality control, maintaining the cellular homeostasis and apoptosis. Dynamin-related protein 1 (Drp1), a member of the dynamin superfamily of proteins, is necessary for the mitochondrial<sup>9</sup> and the peroxisomal<sup>17</sup> division but its precise involvement in the fission pathway is clear.

The mitochondrial fission is preceded by the formation of a prestricted tube-like intermediate, whose dimensions range from 10-400 nm in width<sup>11,54</sup>. This prestriction is marked by the ER-mitochondria contact sites<sup>33</sup> and is thought to be actin dependent<sup>12</sup>. Reconstitution studies till date indicate that Drp1 can self-assemble and polymerize on the membranes to attain a prestricted state, thus tubulating the liposomes and GUVs and constricting membrane tethers pulled from GUVs, but that it is unable to catalyze membrane fission<sup>19,21,25-27,77</sup>. The current model proposes a cooperation between the mitochondrial and classical dynamins, and that neither alone is sufficient for the mitochondrial fission<sup>13</sup>.

However, the recent reports suggest that dynamin-2 knockout having little effect on the mitochondrial morphology as compared to Drp1 knockout<sup>44,45</sup> thus making the role of Drp1 in mitochondrial fission unclear. This study involves investigating Drp1's sufficiency in catalyzing the membrane fission.

### 3.2 Materials and Methods

#### 3.2.1 Cloning, expression, purification and fluorescent labeling of proteins

Human Drp1 Isoform 3 (gift from Richard Youle, Addgene plasmid #45160), Drp1 Isoform 3 (K38A) (a gift from Alexander van der Blik Addgene plasmid #45161), fly (Dynamin-related protein 1, Isoform A, UniProt ID Q9VQE0, a gift kind from Richa Rikhy), yeast (Dynamin-related protein, UniProt ID Q09748, a kind gift from Isabelle Jourdain) and orthologs as well as the point mutants of Drp1 (a kind gift from Jean-Claude Martinou) were cloned with an N-terminal 6xHis-tag and C-terminal SterpII tag in pET15b vector using PCR based seamless cloning<sup>78</sup>. mEGFP



was cloned at N- and C-terminus of Drp1 Isoform 3 to generate GFP-Drp and Drp-GFP respectively. The B-insert of Drp1 Isoform 3 (UniProtID O00429-4, residues 502-599) was cloned with an N-terminal 6xHis-tag followed by mEGFP and C-terminal SterpII tag in pET15b. All the clones were confirmed using DNA sequencing.

Proteins were expressed in BL21(DE3) in autoinduction medium (Formedium, UK) at 18°C for 30-36 h. Cells were pelleted and stored at -40°C. For purification, the frozen bacterial pellet was resuspended in high salt buffer consisting of 20mM HEPES pH 7.4, 500mM NaCl and supplemented with protease inhibitor cocktail (Roche). After resuspension, the cells were lysed by sonication in an ice water bath. The lysate was spun down at 18,500g for 30 mins and the supernatant was incubated with His-Pur cobalt resin (Thermo Scientific) for 1 hour at 4°C. The supernatant was then poured in the PD-10 column, and the resin was washed with 100 ml of HBS buffer (20mM HEPES pH7.4, 150mM NaCl) to get rid of non-specifically bound proteins. Protein was eluted using 20mM HEPES, 150mM NaCl, 250mM Imidazole pH7.4 containing buffer.

Elution was applied to 5 ml Sterptactin column (GE Lifesciences), washed with HBS buffer to get rid of non specifically bound proteins. Protein was eluted using 20mM HEPES pH7.4, 150mM NaCl, 1mM DTT buffer containing 2.5mM desthiobiotin (Sigma). Purification using such tandem affinity ensures full-length and pure preparation of protein as described earlier<sup>63</sup>. For short-term storage (about a week), proteins were kept on ice at 4°C. Proteins were spun down at 100,000g for 20 mins to remove aggregates before biochemical or any microscopy-based assay. For long-term storage (3 months) proteins were stored in high salt containing buffer (20mM HEPES pH7.4, 300mM NaCl, 1mM DTT, 10% glycerol), flash frozen in liquid nitrogen and stored at -80°C.

Protein stored in high salt were dialyzed overnight at 4°C against 20mM HEPES pH7.4, 150mM NaCl supplemented with 1mM DTT and spun down at 100,000g for 20 mins to remove any aggregates before use. Before labeling proteins with thio-reactive Alexa488 C5 maleimide dye (Invitrogen, Life Technologies), proteins were dialyzed overnight at 4°C against 20mM HEPES pH7.4, 150mM NaCl and then labeled with 10 fold molar excess of dye for 1 hour at room temperature and then quenched with 1 mM DTT. Excess of free dye was removed by dialysis. The

labeled protein was resolved on 10% SDS gel and then judged to be free of unreacted dye, which typically migrates at the dye front. The degree of labeling typically achieved under these conditions was 1:1 of protein:dye (mol/mol).

### 3.2.2 GTPase Assay

DOPC (1,2-dioleoyl-sn-glycero-3-phosphocholine) and Cardiolipin (E. Coli) purchased from Avanti Polar Lipids, were aliquoted (75:25 mol%) into a clean glass test tube, dried in vacuum for 30 mins, and hydrated in 20 mM HEPES pH 7.4, 150 mM KCl buffer for 1 hr at 50 °C. The liposomes were extruded through 100-nm pore size filters (Avanti Polar Lipids). Drp1 (1  $\mu$ M) was mixed with nucleotides (Jena Biosciences, Germany) (1 mM) in the absence or presence of liposomes (100  $\mu$ M) in 20 mM HEPES pH 7.4, 150 mM KCl, 1 mM MgCl<sub>2</sub> and incubated at 37°C. Aliquots were taken out at regular intervals and quenched with 5 mM EDTA. The inorganic phosphate released was assayed with the malachite green reagent according to <sup>79</sup>.

### 3.2.3 Supported Membrane Templates (SMrT)

Supported Membrane Templates were prepared as described in chapter 2. After preparing SMrT, the flow cell was equilibrated in filtered 20 mM HEPES pH 7.4, 150 mM KCl (HKS buffer) buffer supplemented with oxygen scavenger cocktail which consists of 0.035mg/ml catalase (Sigma, C-40), 0.2mg/ml glucose oxidase (Sigma, G-2133), 4.5mg/ml glucose (Sigma) and 1mM DTT. In addition to this buffer was also supplemented with 1mM GTP and 1mM MgCl<sub>2</sub>.

Drp1 was dialyzed overnight against HKS and spun down at 100,000g to remove aggregates. Drp1 was then reconstituted in HKS to the final concentration of 1 $\mu$ M and then flowed in the presence of 1mM MgCl<sub>2</sub> and 1mM GTP in the flow cell at low flow rates.

### 3.2.6 Image and statistical analysis, reproducibility

Image analysis was carried out using Fiji<sup>60</sup>. Statistical analysis was carried out using GraphPad Prism (version 5.0a).  $n_{\text{SLB}}$  or  $n_{\text{tube}}$  refers to the number of SLBs or tubes analyzed in a single SMrT preparation.  $N_{\text{SMrT}}$  refers to the number of independent SMrT preparations. N refers to the number of independent experiments.

### 3.3 Results

#### 3.3.1 Biochemical characterization of Drp1

In order to test the sufficiency of Drp1 dependent membrane fission, recombinant Drp1 was purified using the N-terminal 6xHis-tag and the C-terminal SterpII tag (Figure 3.1 A). To test whether Drp1 was functionally active, the GTPase assay (Malachite green assay described in materials and methods) was performed in the absence and presence of liposomes. In the absence of liposomes, Drp1 displayed basal GTPase activity of  $1.2 \pm 0.05 \mu\text{M Pi release}\cdot\text{min}^{-1}$  (basal activity), which got stimulated to  $7.3 \pm 0.27 \mu\text{M Pi release}\cdot\text{min}^{-1}$  in the presence of 25mol% cardiolipin (CL) containing liposomes. Thus in the presence of CL liposomes, the GTPase activity got stimulated 8 folds (Figure 3.1 B).

In order to visualize Drp1's distribution on the membrane, its fluorescent tagging was essential. The functionality of these fluorescently tagged Drp1 construct was accessed using the GTPase assay containing CL liposomes. Labeling Drp1 with thio-reactive Alexa-fluorophore (Ax488-Drp1) led to a complete loss in assembly-stimulated GTPase activity (Figure 3.1 C). Surprisingly, the N-terminally GFP tagged Drp1 construct showed high basal GTPase activity, which did not get stimulated in the presence of liposomes (Figure 3.1 C). In contrast, C-terminally GFP tagged Drp1 showed assembly-stimulated GTPase activity, which was lower than the wild-type (Figure 3.1 C). Since C-terminally GFP tagged Drp1 was the only construct that showed assembly-stimulated GTPase activity, it was used in further experiments but only after mixing with an equimolar amount of wild-type protein, hereafter referred to as Drp1± GFP.

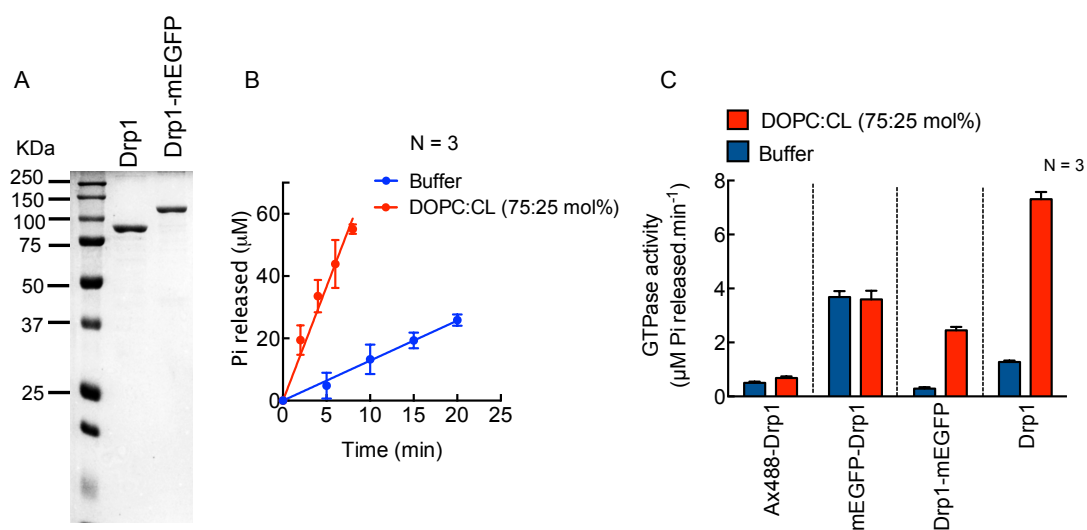


### Figure 3.1 Biochemical characterization of Drp1

(A) 12% Coomassie Brilliant Blue-stained SDS-PAGE of purified Drp1 and Drp1-mEGFP. (B) The GTPase activity of Drp1 in the absence and presence of 100 nm extruded 25mol% cardiolipin-containing liposomes. The data represent mean  $\pm$  S.D for  $n = 3$  experiments. (C) Comparison of GTPase activity of various fluorescently tagged Drp1 constructs with and without 100nm-extruded 25mol% cardiolipin-containing liposomes. The data represent mean  $\pm$  S.D and is analyzed from  $n = 3$  separate experiments.

#### 3.3.2 Drp1 membrane binding and self-assembly

Supported membrane templates with DOPC:CL:*p*TxRed-DHPE (74:25:1 mol%) were incubated with Drp1 $\pm$ GFP alone (“apo” state) or with GDP or with GMP-PNP, a non-hydrolysable analog of GTP for 10 minutes and excess of unbound protein was washed off (Figure 3.2 A, B and C). Surprisingly, under these conditions Drp1 displayed a preferential binding to the tubes as compared to SLBs, implying an intrinsic preference of Drp1 for binding to the regions of high curvature (Figure 3.2 D). In the presence of GDP and the apo-state Drp1 $\pm$ GFP was localized uniformly on the tubes (Figure 3.2 E), while in the presence of GMP-PNP, Drp1 $\pm$ GFP was clustered (Figure 3.2 E). While all the tubes didn’t show this clustering, it was not dependent on the tube size (Figure 3.1 D, GMP-PNP panel). We are unsure of this variability in the Drp1 $\pm$ GFP distribution. Of the tubes where Drp1 $\pm$  GFP showed clusters, they seem to reduce the underlying tube fluorescence (Figure 3.2 E). This effect that Drp1 $\pm$ GFP has in the presence of GMP-PNP is also apparent in the Pearson’s correlation coefficient analysis of Drp1 $\pm$ GFP and membrane fluorescence, where the apo and GDP bound state showed little correlation while the GMP-PNP showed values ranging from no correlation to significantly negative correlation (Figure 3.2 F).

A decrease in the tube fluorescence signifies constriction since the membrane tube is diffraction limited. This observation is consistent with the differences seen in cryo-EM reconstitution of Drp1 in apo and GMP-PNP bound states<sup>21,23</sup>.

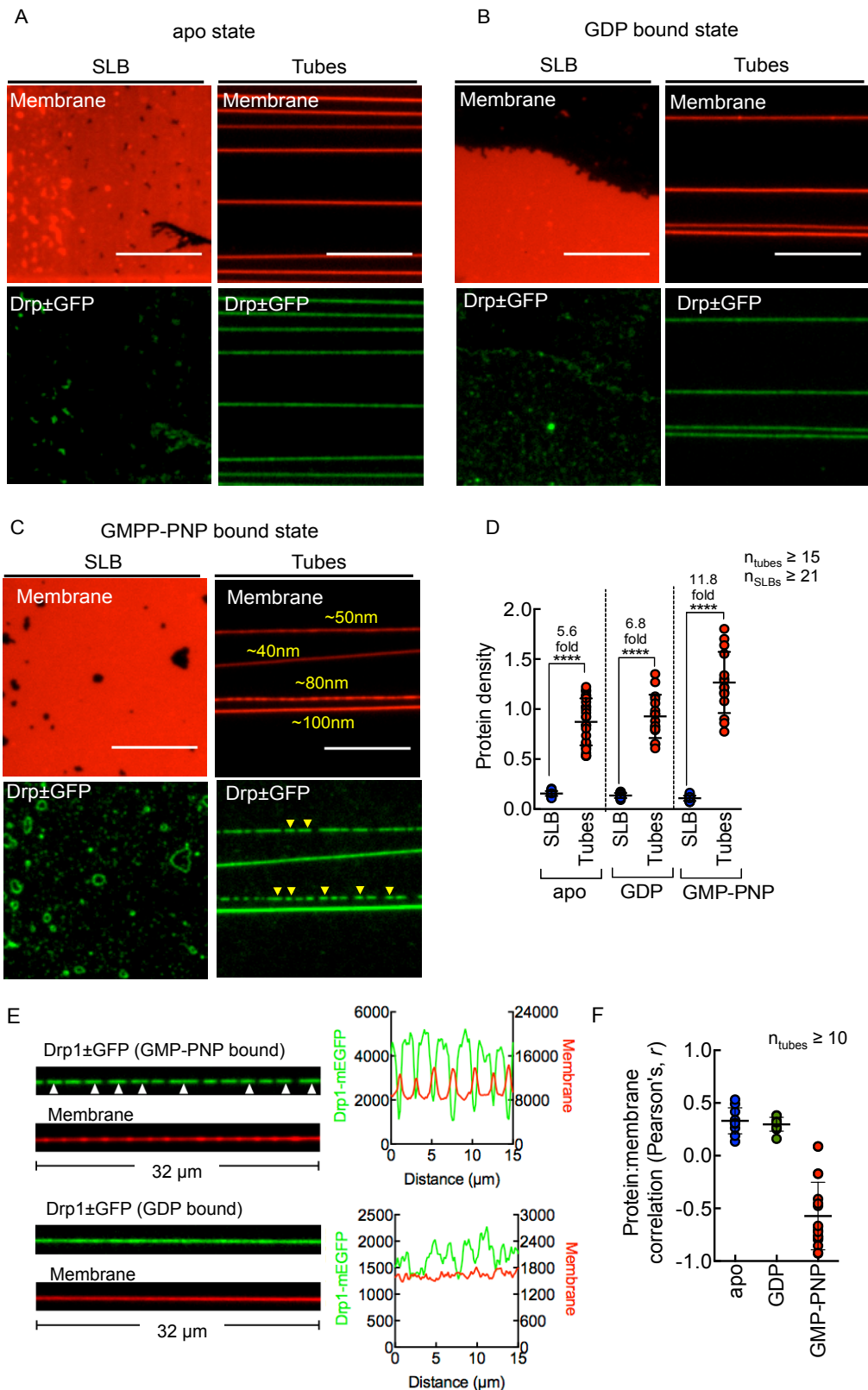


**Figure 3.2 Self-assembly of Drp1 on the membrane tubes**

Representative images of the membrane channel and corresponding Drp1±GFP fluorescence on the Supported Lipid Bilayer (SLBs) and tubes in the apo (A), GDP-bound (B) and GMP-PNP-bound states (C). Scale bar = 10  $\mu\text{m}$ . Yellow arrowheads mark the clusters of Drp1±GFP in the GMP-PNP bound

states on the tubes. (D) Ratios of Drp1±GFP to the membrane fluorescence on the SLB and tubes in the apo, GDP and GMP-PNP, \*\*\*\* indicates  $p < 0.0001$  calculated using Mann-Whitney test. The data represent mean ± S.D; the number of tubes and SLBs analyzed is indicated by  $n_{\text{tubes}}$  and  $n_{\text{SLBs}}$  respectively. (E) Representative image of a single tube. Drp1±GFP in GMP-PNP and GDP bound state. White arrowheads mark the clusters of Drp1±GFP in GMP-PNP bound states. Also associated are the line profiles showing Drp1±GFP distribution in both these states. (F) Pearson's correlation coefficient between Drp1±GFP and membrane fluorescence in different nucleotide-bound states. The data represent mean ± S.D; the number of tubes analyzed is indicated by  $n_{\text{tubes}}$ .

### 3.3.3 B-insert: The membrane-binding site in Drp1

The Pleckstrin-homology domain in classical dynamin regulates its binding to phosphatidylinositol-4,5-bisphosphate on the plasma membrane<sup>80</sup>, similarly, the B-insert region is proposed to regulate the membrane binding of Drp1<sup>21</sup>. Deletion of the B-insert leads to a hyperfused mitochondrial morphology in cells due to a defect in Drp1 recruitment to the mitochondria<sup>19</sup>. Also, studies involving mutations in the critical lysine cassette of the B-insert region demonstrated reduced binding of the Drp1 mutant to the liposomes<sup>75</sup>. In order to test if indeed the B-insert alone can bind lipids independently, a minimal construct of the B-insert (Isoform 3, amino acid residues 502-599) fused to GFP at N-terminus was designed (Figure 3.3 A).



**Figure 3.3 Design of the minimal B-insert construct**

(A) Schematic of the minimal construct used to study Drp1 B-insert (Isoform 3) binding to the supported membrane templates. The construct has an N-terminus mEGFP tag to aid its visualization.

The B-insert was purified using same tandem affinity purification technique as described for Drp1 (materials and methods). When purified B-insert of Isoform 3 was flown on the SMrT containing 25 mol% CL, (excess unbound protein washed off), it got recruited to the membrane tubes (Figure 3.4 A).

Interestingly, the B-insert itself showed a curvature preference in binding to the tubes as compared to the planar supported bilayer (Figure 3.4 A, B). Binding of the protein to a particular lipid can be primarily because of the negative charge

density of the lipid head group or due to specific recognition of a particular lipid. In order to probe if the B-insert interaction is negative charge density dependent or is specific to CL, it was flown on SMrT made of 50% DOPS which would have an equivalent charge density as displayed by 25 mol% CL. Surprisingly, the B-insert also had a preference of binding to CL as compared DOPS on tubes (Figure 3.4 C).

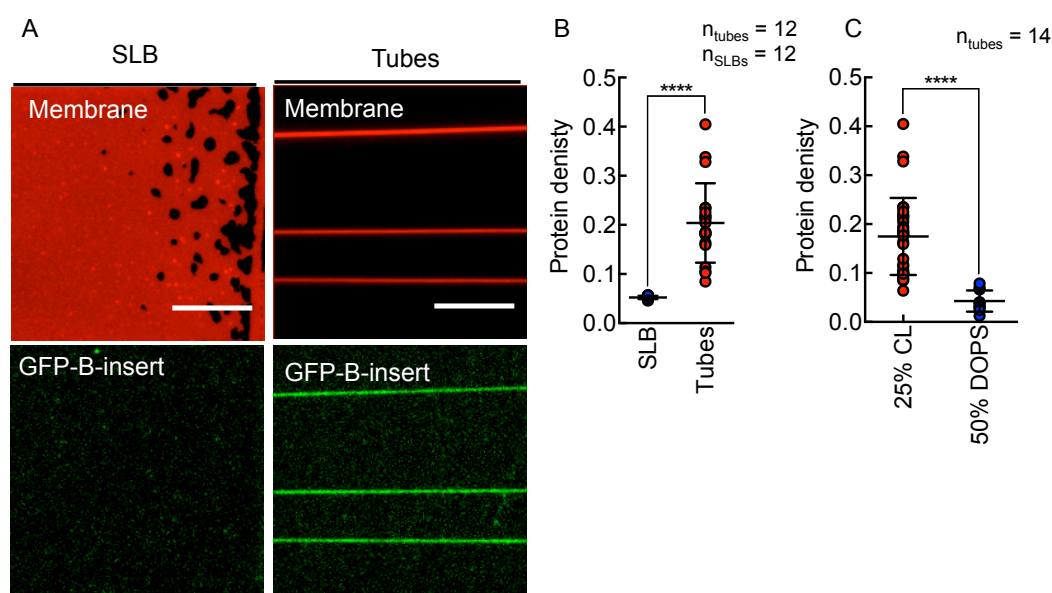


**Figure 3.4 B-insert: The membrane recruitment site in Drp1**

(A) Representative images of GFP-B-insert binding to the supported lipid bilayer (SLBs) and tubes. Scale bar = 10  $\mu\text{m}$ . (B) Ratio of GFP-Drp1-B-insert (Isoform 3) fluorescence to the membrane fluorescence across SLBs and tubes, the data represent mean  $\pm$  S.D; the number of tubes and SLBs analyzed is indicated by  $n_{\text{tubes}}$  and  $n_{\text{SLBs}}$  respectively, \*\*\*\* indicates  $P < 0.0001$  calculated using Mann-Whitney test. (C) The ratio of GFP-Drp1-B-insert (Isoform 3) to membrane fluorescence protein was compared across tubes with different lipid composition, \*\*\*\* indicates  $P < 0.0001$  calculated using Mann-Whitney test. The data represent mean  $\pm$  S.D; the number of tubes analyzed is indicated by  $n_{\text{tubes}}$ .

### 3.3.4 Drp1-catalyzed membrane fission

A recent report demonstrated Drp1 forming spiral structures in the presence of GMP-PNP, a non-hydrolyzable analog of GTP, while in the presence of GTP, Drp1 formed ring-like intermediates<sup>23</sup>. Moreover, recent cryo-EM of Drp1 with MiD49 adaptor protein revealed that GTP hydrolysis leads to curling of the Drp1 spirals to ring-like intermediates<sup>24</sup>. To analyze if such conformational change in response to GTP-hydrolysis has an effect on membrane remodeling ability of Drp1, it was flown with GTP on the supported membrane templates. Remarkably, this led to dramatic

fission of the membrane tubes (Figure 3.5 A, red arrowhead). However, very thick tubes did not undergo fission (Figure 3.5 A, yellow arrowhead). A systematic analysis of the tube radii revealed that the membrane fission is sensitive to the starting tube radius. Tubes under starting tube radius of 200 nm showed a high fission probability, those that had tube radius ranging from 200-250 nm showed a lower fission probability, while those which had radius above 250 nm were resilient to fission (Figure 3.3 B, red trace). Thus Drp1 seems to be self-sufficient in catalyzing fission of the membrane tubes having a wide range of radii distribution.

Recently it was proposed that Drp1 collaborates with Dnm2 (classical dynamin-2) to catalyze mitochondrial division<sup>13</sup>. When Dnm2 fission activity was independently tested out on the same assay system, it was found to be less effective in comparison to Drp1 (Figure 3.5 B, blue trace). Although tubes below 50 nm showed fission activity with Dnm2, it was with lower probability as compared to Drp1, while tubes above 50 nm were completely resistant to fission (Figure 3.5 B, blue trace). In order to further analyze Drp1 mediated membrane fission tubes ranging from 10-50nm radii that showed a robust fission activity were used. The GTPase defective Drp1 mutant K38A<sup>9</sup>, Drp1 mutant in the lysine cassette of the B-insert region (K557A; K506A and K569A; K571A)<sup>75</sup> in Drp1 and the Drp1 mutant in the stalk domain A395D<sup>81</sup> were severely or completely defective in catalyzing membrane fission under identical experimental condition (Figure 3.5 C). Remarkably, Drp1-catalyzed membrane fission activity was seen to be evolutionarily conserved across both yeast and *drosophila* orthologs as they both showed robust fission activity in the presence of GTP (Figure 3.5 D).



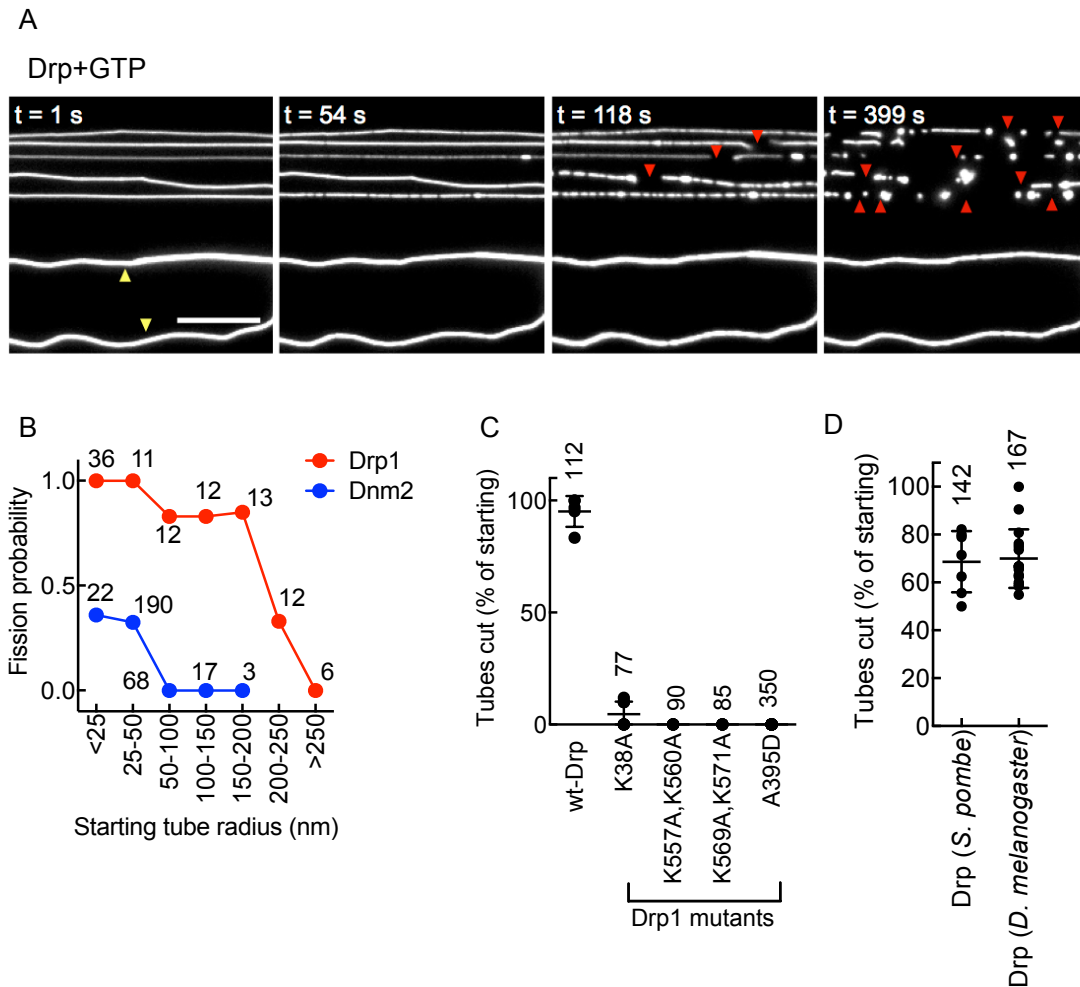


### Figure 3.5 Drp1-catalyzed membrane fission

(A) Stills from the time-lapse movie acquired while flowing Drp1 in the constant presence of GTP, showing Drp1-catalyzed fission. Yellow arrowheads mark uncut tubes, red arrowhead mark site of fission. Scale bar = 10  $\mu\text{m}$ . (B) Drp1 and Dnm2 fission probability plotted as a function of starting tube radius. The number of tubes analyzed in each size range is indicated in the plot. (C) Analysis of different Drp1 mutants in fission assay, the data represent mean  $\pm$  S.D; the total number of tubes analyzed across different fields is indicated above each data set. Each point in the data set represents an average number of tubes cut per field. (D) Analysis of Drp1 ortholog in *S. pombe* and *D. melanogaster* in the SMrT, the data represent mean  $\pm$  S.D; the total number of tubes analyzed across different fields is indicated above each data set. Each point in the data set represents an average number of tubes cut per field.

#### 3.3.5 Mechanism of Drp1-catalyzed membrane fission

In order to decipher the mechanism of membrane fission, Drp1 was first preassembled in the GMP-PNP bound state and allowed to form the scaffolds that caused constriction of the underlying membrane (Figure 3.6 A, referred to as

preassembled Drp1, marked by white arrowheads and Figure 3.6 B, line profile in the blue trace). GTP was then flown on the preassembled Drp1 scaffolds. Tubes that showed the constriction were focused to access the effect of GTP-hydrolysis on the Drp1 scaffolds. Interestingly, GTP arrival led to a further constriction of membrane tubes (Figure 3.6 A, t = 7 sec) finally causing membrane fission (Figure 3.6 A, t = 8.7 sec, Figure 3.6 B, line profile in the red trace). On wide tubes that were fission resistant (Figure 3.5 A and B), Drp1 addition with GTP leads to a cycle of decline and recovery of membrane fluorescence thus indicating the underlying membrane tube undergoing constriction and release cycles (Figure 3.6 D, the constriction is indicated by yellow arrowheads). While on fission compliant tubes, membrane fission was preceded by prominent constriction (Figure 3.6 C, the constrictions are indicated by yellow arrowheads, while the fission events are marked by red arrowhead). Thus, Drp1 in response to the GTP hydrolysis constricts the membrane further leading to fission but fails to cut thick tubes.

Membrane fission could take place either underneath (see schematic in Figure 3.6 F) or at the edge of the Drp1 scaffold (see schematic in Figure 3.6 E). If the fission occurred underneath the Drp1 scaffold, it would translate into the splitting of the scaffold while if fission occurred at the edge of the scaffold, it would leave the scaffold intact (Figure 3.6 F and E). Monitoring the response of addition of GTP to preassembled Drp1± GFP in both the membrane and protein channel indicated that out of total 35 single fission events analyzed, 26 showed an intact scaffold while 9 events showed scaffold splitting. This process is in contrast to the classical dynamin, which undergoes fission exclusively under the scaffold <sup>64</sup>.

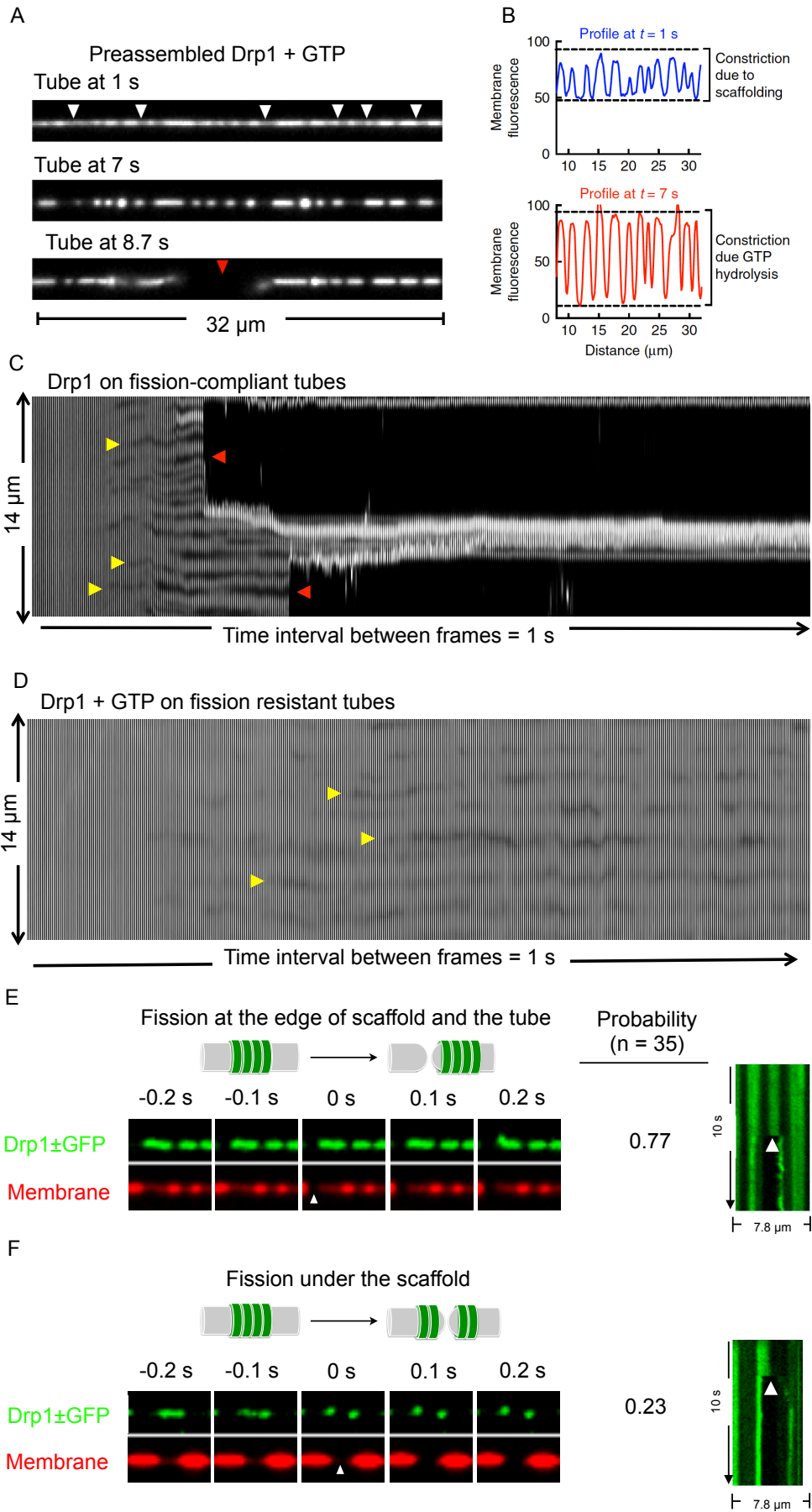


### Figure 3.6 Mechanism of Drp1-catalyzed membrane fission

(A) Stills from the time-lapse movie showing the effect of GTP addition to preassembled Drp1 scaffolds in the presence of GMP-PNP. White arrowheads mark the site of Drp1 mediated constriction. (B) Line profile of tube fluorescence at the indicated time points. (C) Montage of single tube undergoing fission, yellow arrowheads mark the site of constriction while red arrowheads mark the site for fission. (D) Montage of a single thick tube that does not undergo fission, yellow arrowheads mark site of constriction. (E) Schematic for membrane fission occurring at the edge of the Drp1 scaffold (Schematic prepared by Thomas Pucadyil). Frames from time-lapse imaging form dual channel movie showing the distribution of Drp1±GFP (green) and tube underlying Drp1 scaffold (red). Also included is kymograph (protein channel) white arrowhead mark the site of fission. The probability of these events occurring is indicated. (F) Schematic for membrane fission occurring underneath Drp1 scaffold (Schematic prepared by Thomas Pucadyil). Frames from time-lapse imaging form dual channel movie showing the distribution of Drp1±GFP (green) and tube underlying Drp1 scaffold (red). Also included is kymograph (protein channel) white arrowhead mark the site of fission. The probability of these events occurring is indicated.

### 3.4 Discussion

The results from this study reveal that Drp1 is self-sufficient to catalyze membrane fission of tubes as wide as 500nm. These results differ from the earlier reports<sup>19,21,25</sup> possibly due to the assay system of membrane tubes used here which better mimic the mitochondrial morphology and a prudent choice of the fluorescent construct which shows a stimulated GTPase activity. Alternatively, these differences could also result from the intrinsic differences between Drp1 Isoforms used in the earlier studies<sup>26,27,77</sup>, as various Isoforms may exhibit differences in the GTP hydrolysis and binding<sup>75</sup>. Even though Drp1 orthologs in *yeast* and *D. melanogaster* are quite different as compared to the mammalian Drp1, the fission activity seems to be evolutionarily conserved. These results reiterate the universal role of Drp1 as a membrane fission catalyst.

Drp1's membrane binding is nucleotide-independent but remarkably curvature-sensitive, as it prefers to bind to tubes (high curvature) as opposed to the planar supported lipid bilayer. Surprisingly, the B-insert (the membrane binding region of Drp1) was also found to be curvature sensitive, which might augment Drp1's curvature preference. In response to GTP-binding, Drp1 seems to self-assemble in the form of scaffolds, which constrict the underlying membrane to a

variable extent. Drp1 requires GTP-hydrolysis for membrane fission, which on longer time scales might also serve for disassembly of the scaffold.

Various different studies have indicated the importance of mitochondrial constriction just prior to fission. The role of ER tubule in marking the site for the mitochondrial fission<sup>33</sup> and role of actin-mediated mitochondrial constriction<sup>39,82,83</sup> is well established. Indeed Drp1 was found to be restricted in fission of very thick tubes (above 500nm diameter), possibly explaining the requirement of a prior mitochondrial constriction step.

Although dynamin-2 can catalyze fission, it seems to be severely restricted in membrane fission activity on tubes of larger dimensions. These differences between mitochondrial and endocytic dynamins may reflect the differences in the substrates on which they act. While dynamin-2 severs 20 nm neck of endocytic pits<sup>84</sup>, Drp1 has to mediate fission of 20-400 nm wide constricted mitochondria<sup>33,54</sup>. Additionally, these differences forefend the possibility that Drp1 is merely acting to remodel and constrict mitochondria<sup>85</sup>.

## **Chapter 4**

# **Role of the mitochondrial adaptor proteins in Drp1-catalyzed membrane fission**

## 4.1 Introduction

Several single pass transmembrane domain-containing proteins present on the outer mitochondrial membrane function as adaptors to recruit cytosolic Drp1 to the mitochondria<sup>28</sup>. The absence of these adaptors results in a hyperfused mitochondrial phenotype and is attributed to a failure in mitochondrial division caused by insufficient recruitment of Drp1. The Mitochondrial fission factor (Mff)<sup>30,32</sup> and the Mitochondrial dynamics proteins (MiD49 and MiD51, also known as MIEF2 and MIEF1 respectively)<sup>35,86</sup> represent such adaptors in mammals and are reported to act independently of each other<sup>87,88</sup>. While MiD49 and 51 are located solely on mitochondria<sup>87</sup>, Mff is present on peroxisomes as well<sup>17</sup>. Mff has two motifs VPEK and VPER (single letter amino acid codes)<sup>89</sup>, that specifically bind the stalk domain in Drp1<sup>20,89</sup>. MiD49/51 have a defined loop region called the Drp1 recruitment region (DRR) that interacts with the stalk domain<sup>35,90,91</sup>. Curiously, these adaptors mark the site of eventual mitochondrial division<sup>33</sup>. Remarkably, Mff displays a clustered organization on mitochondria that coincide with sites where the mitochondria appear constricted<sup>11,92</sup> independent of Drp1. Similar to Mff, MiD49/51 is also present at sites where the mitochondria appear constricted<sup>93</sup>. Presently, it is unclear if clustering of adaptors causes constriction or if clusters of adaptors partition to constricted regions formed by an unidentified upstream process.

## 4.2 Materials and Methods

### 4.2.1 Cloning, expression and purification of proteins

The cytosolic domains of the Mitochondrial fission factor (Mff $\Delta$ TM) and the Mitochondrial dynamics proteins (MiD49/51 $\Delta$ TM) were kind gifts from Michael Ryan (Monash University). Mff $\Delta$ TM was cloned with an N-terminal StrepII and C-terminal 6xHis-tag in a pET15b vector. MiD49/51 $\Delta$ TM were cloned with an N-terminal 6xHis-tag and C-terminal StrepII tag in a pET15b vector. The 6xHis-tag serves to recruit these proteins in the same orientation as found for the full-length proteins onto a membrane containing the chelator DGS-NTA (Ni<sup>2+</sup>) lipid. For experiments involving Drp1 in these assays, the 6xHis-tag from Drp1 was removed by PCR. A single cysteine residue was introduced at the N terminus of Mff $\Delta$ TM (C-

Mff $\Delta$ TM) to enable labeling with maleimide-containing fluorophores. All clones were confirmed by DNA sequencing. Proteins were expressed and purified as mentioned in the materials and methods section of Chapter 3.

#### **4.2.2 Labeling of Mff with extrinsic fluorophores**

The purified C-Mff $\Delta$ TM was dialyzed overnight at 4°C against 20 mM HEPES pH 7.4 buffer with 150 mM NaCl, spun down at 100,000 g to remove aggregates and labeled with 10-fold molar excess of the thiol-reactive Alexa 488 C5 maleimide dye (Invitrogen, Life Technologies) for 1 hour at room temperature. Reactions were quenched with 1 mM DTT. Excess free dye was removed by dialysis. Labeled C-Mff $\Delta$ TM was resolved on a 15% SDS gel and judged to be free of unreacted dye, which typically migrates with the dye front. The degree of labeling typically achieved under these conditions was 1:1 of protein:dye (mol/mol).

#### **4.2.3 Supported Membrane Templates (SMrT)**

The SMrT were prepared with a varying concentration of cardiolipin and contained 5 mol% of the chelator lipid, 1,2-dioleoyl-sn-glycero-3-[(N-(5-amino-1-carboxypentyl)-iminodiacetic acid) succinyl (nickel salt) (DGS-NTA Ni<sup>2+</sup>) for recruitment of adaptor proteins with a 6xHis-tag.

#### **4.2.4 Membrane tubes with mEGFP selectively localized to the inner leaflet**

Membrane tubes with mEGFP selectively localized to the inner leaflet were prepared using a previously described protocol<sup>57</sup>. Briefly, templates with 5 mol% chelator lipid were hydrated with buffer containing 6xHis-mEGFP. After formation, templates were washed with buffer containing 10 mM EDTA, which removes mEGFP bound to the outer leaflet while retaining the protein bound to the inner leaflet of tubes. Templates were then washed with buffer to remove EDTA and subsequently charged with 10 mM Ni<sup>2+</sup>. Excess Ni<sup>2+</sup> was again washed off with buffer before incubation with Mff.



## 4.3 Results

### 4.3.1 Adaptor proteins facilitate Drp1-catalyzed membrane fission

Various adaptor proteins on the mitochondrial and peroxisomal membrane play a critical role in the recruitment of Drp1<sup>94</sup>. In order to better mimic these organelles, the cytosolic domain of Mff (Mff $\Delta$ TM, Figure 4.1A), MiD49 (MiD49 $\Delta$ TM, Figure 4.1B) and MiD51 (MiD51 $\Delta$ TM, Figure 4.1B) were purified and tethered, via an engineered 6xHis-tag, to SMrT containing 5 mol% of the chelating lipid (DGS-NTA Ni<sup>2+</sup>).

In order to mimic their native orientation, Mff was recruited via a C-terminal 6xHis-tag while MiD49 and MiD51 were recruited via an N-terminal 6xHis-tag (Figure 4.1A and B). SMrT also contained 5 mol% of cardiolipin, a concentration estimated to be present on the outer mitochondrial membrane<sup>67,95</sup>. Templates were first incubated with mimics of the adaptor protein (1  $\mu$ M) and excess unbound adaptor in solution was washed off before passing Drp1. This ensured that Drp1 bound only the membrane-tethered adaptors.

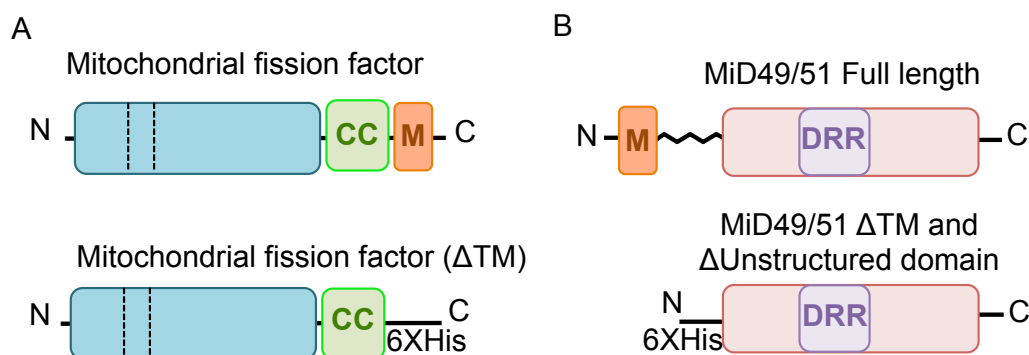


**Figure 4.1 Schematic of Mff, MiD49/51 and their mimics used in Supported Membrane Templates**

(A) Schematic showing the domain architecture of full-length Mitochondrial fission factor (top panel) and a construct with the cytosolic domain used in experiments (bottom panel). Shown are recognition sites for Drp1 (dotted lines), the coiled-coil domain (CC) and the transmembrane domain (M) in full the length Mff. Note that the construct used in experiments has the transmembrane domain replaced with a 6xHis-tag. (B) Schematic showing the domain architecture of full-length MiD49/51 (top panel) and a construct with the cytosolic domain used in experiments (bottom panel). Shown are the transmembrane domain (M), unstructured region (zig-zag line) and the Drp1 recognition region (DRR). Note that the construct used in experiments has the unstructured region deleted and the transmembrane

domain replaced with a 6xHis-tag.

Remarkably, flowing Drp1 with GTP onto Mff-, MiD49- and MiD51-coated tubes, with 5 mol% CL resulted in their fission (Figure 4.2 A, B and C respectively). Importantly, tubes displaying just 5 mol% CL remained unaffected emphasizing that adaptors become necessary to recruit Drp1 for fission on a membrane displaying physiological concentrations of CL (Figure 4.2 D). This is apparent from a plot showing quantitation of tubes cut (Figure 4.2 E).

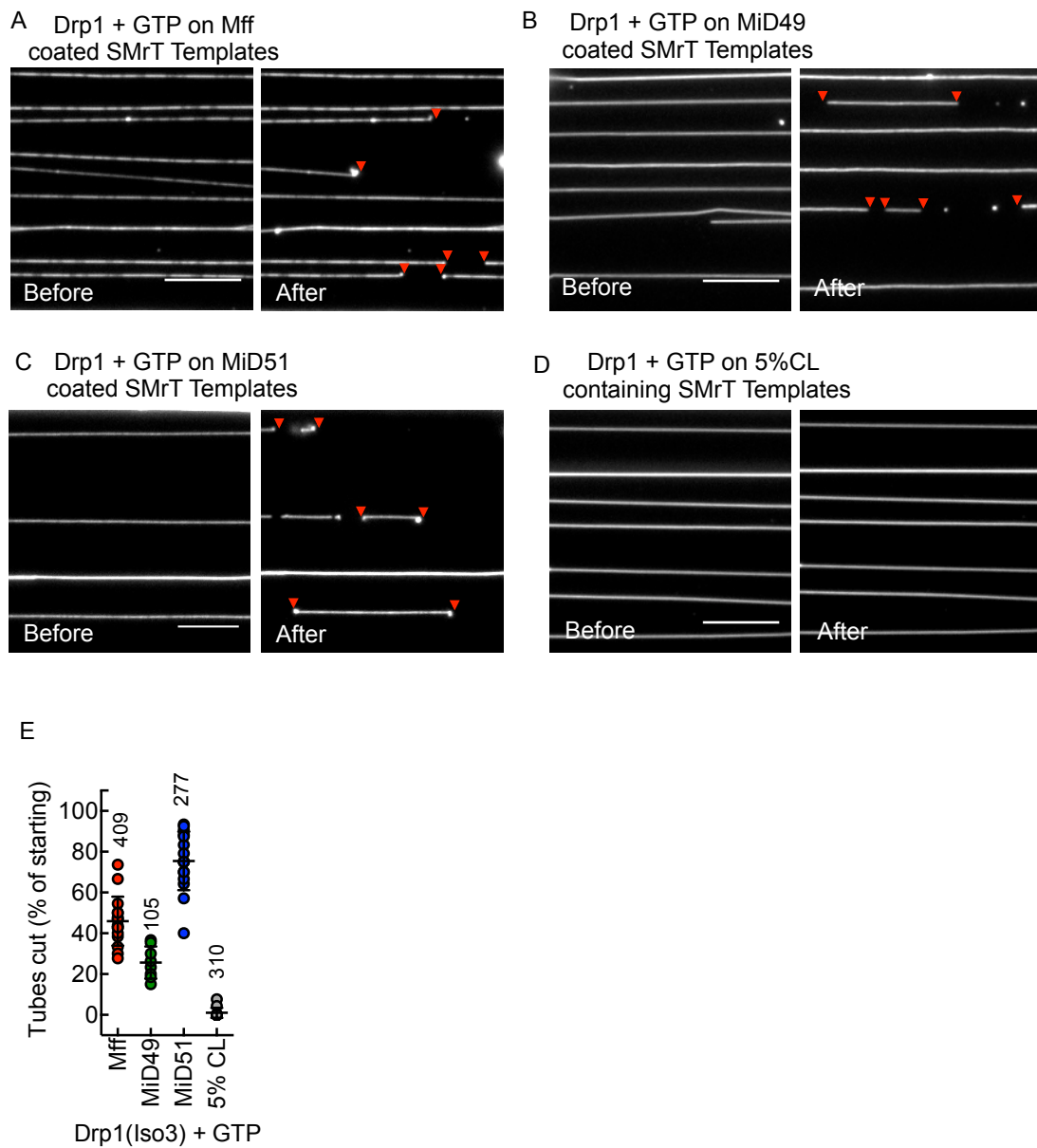


**Figure 4.2 Adaptor proteins facilitate Drp1-catalyzed membrane fission**

Representative images of Drp1 mediated membrane fission on Mff (A), MiD49 (B), and MiD51 (C) coated membrane tubes respectively. MiD51 was flown with ADP since it requires ADP as co-factor for stimulating Drp1's GTPase activity<sup>96</sup>. (The images were acquired after 10 mins of incubation with Drp1 Isoform 3 + GTP, tubes were of membrane composition DOPC:CL:DGS-NiNTA: *p*-TxRed DHPE 89:5:5:1mol%). Red arrowhead in the after field marks site for fission. Scale bar = 10 $\mu$ m. (D) Representative images on flowing Drp1 in the presence of GTP on membrane tubes 5 mol%CL (The images were acquired after 10 mins of incubation with Drp1 Isoform 3 + GTP, tubes were of membrane composition DOPC:CL:DGS-NiNTA: *p*-TxRed DHPE 89:5:5:1mol%). (E) Quantitation of the percentage tube cuts for Drp1 + GTP on Mff, MiD49, and MiD51 coated membrane tubes and supported membrane templates without the adaptor protein. The data represent mean  $\pm$  S.D; the total number of tubes analyzed across different fields is indicated above each data set. Each point in the data set represents an average number of tubes cut per field.

#### 4.3.2 Organization of mitochondrial fission factor on the membrane

Interestingly, unlike MiD49 or MiD51 recruiting Mff to membrane tubes caused the tube fluorescence to appear striated (Figure 4.1 A, Before panel). Our previous work with Drp1 has revealed that a localized dimming of the tube fluorescence coincides with a constriction event. This suggested that Mff could by itself organize to constrict the underlying membrane tube. To further investigate this behavior, we extrinsically labeled Mff with Alexa488-maleimide and passed it on SMrT. Surprisingly, fluorescent Mff displayed a highly clustered distribution, both on tubes and the supported bilayer (Figure 4.3 A). As a control, 6xHis-mEGFP recruited on the membrane, in the same manner, showed a uniform distribution. Mff clusters on coincide with regions of dimmer fluorescence, indicating constriction (Figure 4.3 B, also apparent in the corresponding line profile). To eliminate the possibility that the non-uniform membrane fluorescence was a consequence of changes in the fluorescence properties or differential partitioning of the lipid probe, unlabeled Mff was recruited to membrane tubes with mEGFP selectively tethered to the inner monolayer (Figure 4.3 C, schematic). Under these conditions, regions of dimmer fluorescence coincided with dimmer mEGFP fluorescence thus validating our result that clusters of Mff indeed constrict the underlying membrane tube (Figure 4.3 D, also apparent in the corresponding line profile).

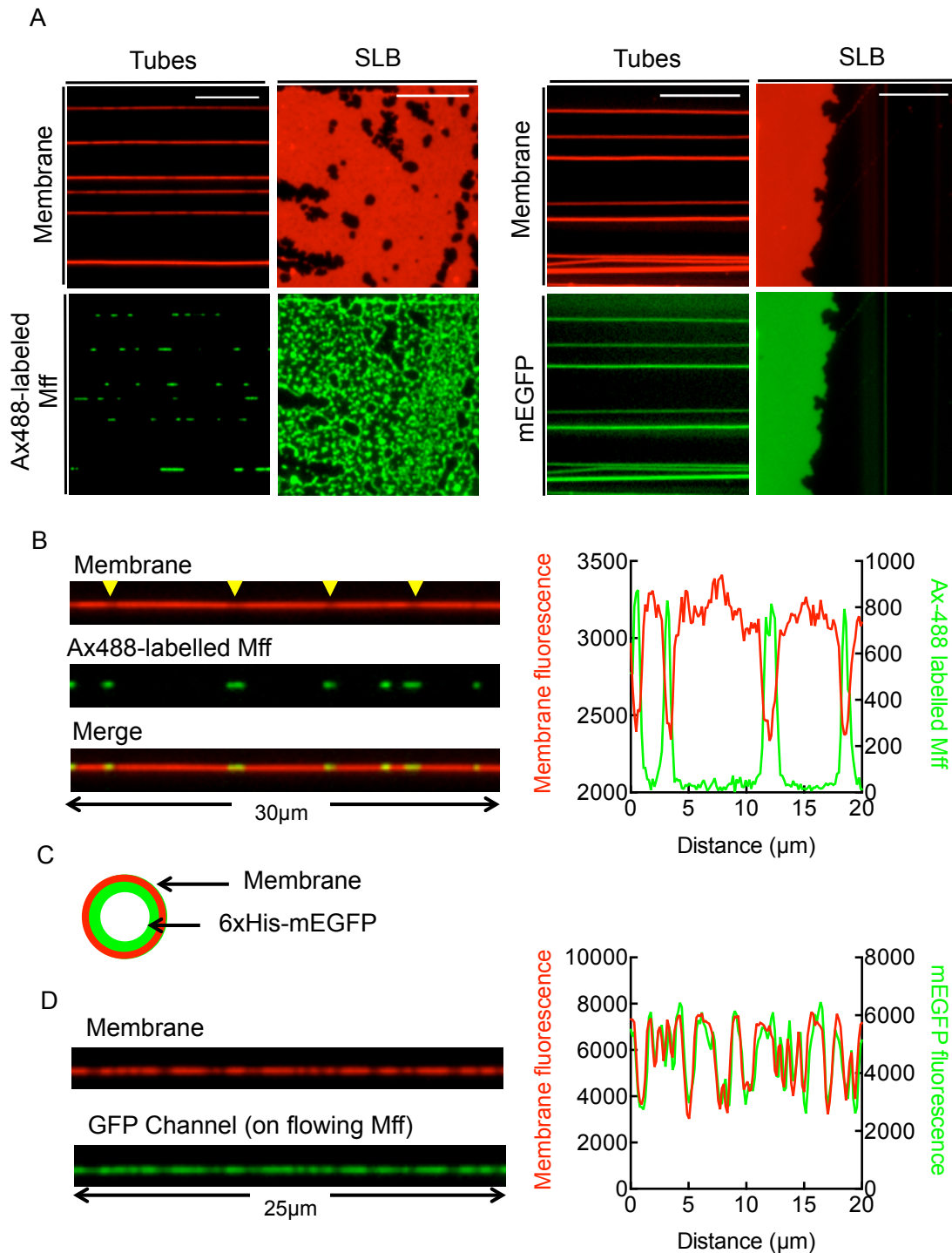


### Figure 4.3 Organization of Mitochondrial fission factor on the membrane

(A) Representative images of membrane-localized Ax488-labelled Mff $\Delta$ TM (left) and mEGFP (right) on membrane tubes and SLBs. Lipid composition of the membrane is DGS-NTA ( $\text{Ni}^{2+}$ ):CL:*p*-TxRed DHPE:DOPC (5:5:1:89 mol%). Scale bar = 10  $\mu\text{m}$ . (B) Representative images of a single tube in the membrane and protein channel (Alexa-488 labeled Mff), yellow arrows indicate sites of constriction. Also shown is the line profile indicating Ax488-Mff distribution on membrane tubes. (C) Schematic showing a cross-section of a membrane tube with mEGFP selectively localized to the inner leaflet. (D)

Representative images of a single tube showing Mff-induced constriction on tubes with mEGFP localized to the inner leaflet. Also shown is a corresponding line profile.

### 4.3.3 Coiled-coil domain of Mff is involved its oligomerization

A study involving Mff  $\Delta$ TM had shown it to be a tetramer in solution<sup>97</sup>, which gets converted to a predominantly monomer population on deletion of a 32 residues-long coiled-coil domain (CCD)<sup>97</sup> (Figure 4.4A).

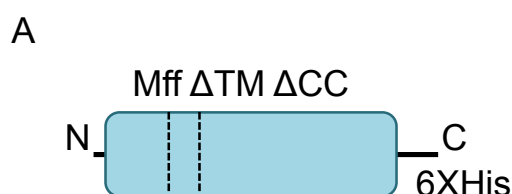


**Figure 4.4 Schematic of Mff with deletion of the coiled-coil and transmembrane domain**

(A) Schematic showing the domain architecture of Mff with the deletion of the transmembrane and the coiled-coil domain.

Interestingly, on deletion of the CCD, Mff $\Delta$ TM did not cluster on tubes and on the supported bilayer (Figure 4.5A). Furthermore, Mff $\Delta$ CCD failed to constrict tubes (Figure 4.5 B), indicating that oligomerization via the CCD is required for Mff's membrane activity.

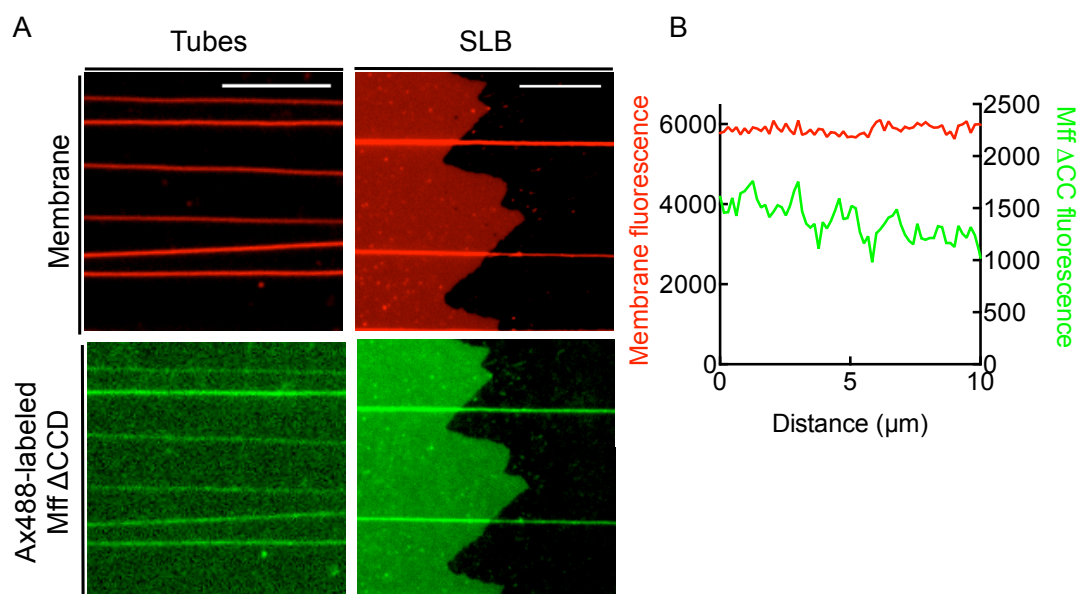


**Figure 4.5 Coiled-coil region involved in the oligomerization and membrane constriction activity of Mff**

(A) Representative images showing localization of Ax488-labeled Mff  $\Delta$ TM  $\Delta$ CC on tubes and SLBs. Scale bar = 10  $\mu$ m. (B) Line profile indicating Ax488-Mff  $\Delta$ CC distribution on membrane tube.

#### 4.3.4 Mff facilitates Drp1 recruitment to the membrane

As observed in Figure 4.2 A, Mff facilitated Drp1-mediated fission of membrane tubes containing 5 mol% CL. In order to investigate if Mff also facilitates Drp1 recruitment to the membrane, Mff was first recruited to the membrane using His-tag and chelating-lipid interaction, the excess unbound protein being washed off. Drp1 $\pm$ GFP was then flown in different nucleotide-bound states, incubated and excess unbound protein was washed, after which protein and membrane channel were imaged. Strikingly, Mff dramatically improved Drp1's membrane binding to the tubes and supported lipid bilayer containing 5 mol % CL (Figure 4.6 A, B). However, Drp1 still showed a preference for binding to the tubes as compared to the supported lipid bilayer (Figure 4.6 C) but to a lesser extent as compared to only CL containing templates (Chapter 3, Figure 3.2 D).

A systematic study of Drp1's fission activity in the constant presence of GTP on a range of CL concentrations on Mff coated Supported Membrane Templates revealed that Mff lowers requirement for CL for fission (comparison of the blue trace, which represents SMrT without Mff and red trace, which represents SMrT with Mff, Figure 4.6 D). In the absence of Mff, Drp1 required a minimum of 20 mol% CL to show fission activity. The presence of Mff changed this requirement, with ~20% of the tubes showing fission events even in the absence of CL.

Interestingly, the presence of Mff led CL dependence to exhibit a biphasic trend with an optimum at 15 mol% CL (see the red trace in Figure 4.6 D).

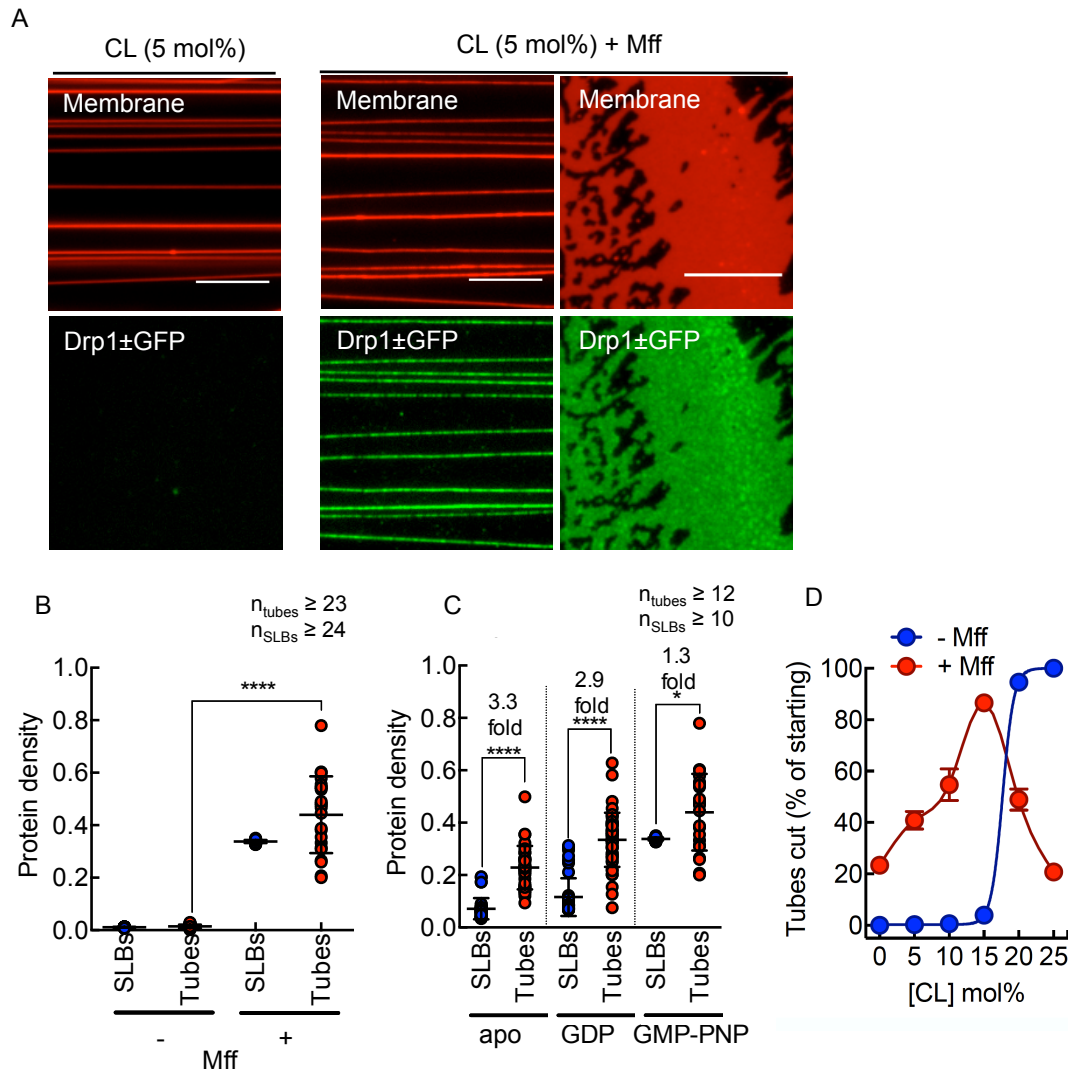


**Figure 4.6 Mff mediated Drp1 recruitment to the membrane tubes and fission**

(A) Representative images of Drp1±GFP on tubes and SLB with 5 mol% CL with and without Mff. Scale bar = 10µm. (B) Ratios of Drp1±GFP and membrane fluorescence in the presence and absence of Mff on 5 mol% CL containing supported membrane templates. The data is represented as mean ± S.D, \*\*\*\* indicates  $p < 0.0001$  calculated using Mann-Whitney's test. The number of tubes and SLBs analyzed is indicated by  $n_{\text{tubes}}$  and  $n_{\text{SLBs}}$  respectively. (C) Ratios of Drp1±GFP and membrane fluorescence under different nucleotide-bound states on the SLB and tubes. The data is represented as mean ± S.D, \*\*\*\* indicates  $p < 0.0001$ , while \* represents  $p < 0.013$  calculated using Mann-Whitney's test. The number of tubes and SLBs analyzed is indicated by  $n_{\text{tubes}}$  and  $n_{\text{SLBs}}$  respectively. (D) Plot showing the percentage of tubes cut as a function of cardiolipin concentration. Red trace indicates tubes with Mff while blue trace indicates tubes without Mff. The data represent mean ± S.E.M.,  $n_{\text{tubes}}$  is greater than 50 for each condition.

#### 4.4 Discussion

The presence of Drp1 adaptor proteins (Mff, MiD49, and MiD51) independently aids Drp1 recruitment and fission on supported membrane templates. Our results indicate that co-incident display of Drp1 adaptor proteins and cardiolipin can wield a significant influence on the Drp1's membrane recruitment. Importantly, once recruited on the membrane, Drp1 can act as a minimal machinery to catalyze membrane fission. Since Drp1's binding partners are constitutively present on the outer mitochondrial membrane, their localization could potentially mark the site for mitochondrial and peroxisomal division by recruiting Drp1. In light of this, Mff's property to self-oligomerize in the form of clusters on the membrane surface and subsequent membrane remodeling could determine the site of mitochondrial division. Mff also synergizes with cardiolipin for Drp1 recruitment and fission. Interestingly, Drp1 also led to fission of Mff-coated tubes without cardiolipin, which suggests that cardiolipin is not an absolute requirement for membrane fission. Also, Mff led to Drp1's dependence for cardiolipin to show a biphasic trend for fission activity, optimum being at 15 mol % CL thus implying that cardiolipin might not be an absolute requirement for fission but depending on its concentration can facilitate or inhibit fission.

Although not a part of this study, another critical aspect is the localization of MiD proteins on the membrane surface. It would be interesting to see whether there is cross-talk between different adaptor proteins present on the membrane surface, as they all seem to localize at the site of mitochondrial division<sup>93</sup>. These adaptor proteins apart from marking the site for mitochondrial division might also recruit factors other than Drp1 that would facilitate initial mitochondrial constriction.

Since Drp1 fission activity seems to be intrinsically regulated by membrane tube dimensions, it necessitates an upstream constriction event on mitochondrion prior to Drp1 assembly thus defining the role of ER-contact sites on mitochondria. In this regards, it would be interesting to look at the influence of the adaptor proteins on Drp1's ability to sever wider tubes.



**Chapter 5**  
**Functional differences in Drp1 Isoforms**

## 5.1 Introduction

The mitochondrial morphology varies in different tissues; it ranges from short and fragmented to elongated across different cell-types<sup>46</sup>. One possible way to maintain such difference in the morphology is by regulating mitochondrial fission and fusion with the excess division leading to fragmented and the excess fusion causing elongated mitochondria<sup>51</sup>. A potential way to control the size of mitochondria is to regulate the division machinery, including the central player Drp1 and its adaptors. A recent report suggests that Mff-dependent Drp1 fission is differentially regulated to maintain short mitochondria in the axon, as opposed to the elongated mitochondria seen in dendrites<sup>98</sup>. Drp1 has eight known isoforms that arise from alternative splicing and are expressed in a tissue-specific manner<sup>99</sup>. Interestingly, the surface plasmon resonance-based analysis revealed Drp1 Isoform 1, 2 and 3 to display distinct lipid-binding properties.

Apart from the mitochondrial division, Drp1 is also involved in the peroxisomal division<sup>17</sup>. The overexpression of Drp1 mutant defective in GTP hydrolysis (K38A) resulted in elongated peroxisomes<sup>17</sup>. Interestingly, a study involving overexpression of Isoform 1 showed elongated peroxisomes as opposed to overexpression of Isoform 3 which resulted in fragmented peroxisomes<sup>100</sup>. Together, all these observations highlight the functional differences in Drp1 Isoforms.

## 5.2 Materials and methods

### 5.2.1 Cloning, expression, purification and fluorescent labeling of proteins

Human Drp1 Isoform 1 and 2 (a kind gift from Jean-Claude Martinou) were cloned with an N-terminal 6xHis-tag and C-terminal SterpII tag in pET15b vector using PCR based seamless cloning<sup>78</sup>. The mEGFP was cloned at C-terminus of Drp1 Isoform 1 to generate Drp-GFP construct. The B-insert of Drp1 Isoform 1 (UniProtID O00429-1, residues 502-636) and Isoform 3 (UniProtID O00429-4, residues 502-599) were cloned with an N-terminal 6xHis-tag followed by mEGFP and C-terminal SterpII tag in pET15b. All clones were confirmed using DNA sequencing.

### 5.2.2 Supported Membrane Templates (SMrT)

The Supported Membrane Templates were prepared with 5 mol% of

cardiolipin, chelator lipid, 1,2-dioleoyl-sn-glycero-3-[(N-(5-amino-1-carboxypentyl)-iminodiacetic acid) succinyl (nickel salt) (DGS-NTA Ni<sup>2+</sup>, 5 mol%) for the recruitment of Mff with 6xHis-tag and 1 mol% of *p*-Texas red DHPE was incorporated to aid visualization of the templates.

A mixture of DOPC, cardiolipin (Avanti Polar Lipids) and *p*-Texas red DHPE (74:25:1 mol%) was aliquoted in a glass vial to make the final concentration of 1mM in chloroform, to make SMrT without chelator lipid.

### **5.2.3 GTPase assay**

GTPase activity was carried out as mentioned in the materials and methods section of chapter 3.

## **5.3 Results**

### **5.3.1 Drp1 Isoform 1 is defective in membrane recruitment and fission on Mff coated supported membrane templates**

Drp1 has various isoforms that show different tissue-specific expression and localization<sup>101,102</sup>. Since different mitochondrial morphology might stem from the differential activity of these multiple isoforms, these were tested out in the supported membrane templates. Drp1 Isoform 1, which is the longest Drp1 Isoform and differs from Isoform 3 only in the B-insert region, was recombinantly expressed and purified (see schematic and the alignment of Drp Isoform 1 with Drp1 Isoform 3 in Figure 5.1 A and B respectively).



**Figure 5.1 Schematic comparing Drp1 Isoforms**

(A) Schematic showing the domain architecture of Drp1, based on its structure<sup>19,75</sup>. Shown is the domain architecture for longest Drp1 Isoform 1. Isoform 3 has 533-569 amino acid residues missing which are indicated by the dotted line. (B) Alignment of Drp1 Isoform 1 (UniProtID O00429-1) and Isoform 3 (UniProtID O00429-4). The sequences were acquired from Uniprot<sup>103</sup> and aligned using Clustal W alignment software<sup>104</sup>.

This Isoform was tested out on Mff coated supported membrane templates containing 5 mol % CL in the constant presence of GTP. Surprisingly, Drp1 Isoform 1 was found to be defective in mediating membrane fission (Figure 5.2 A). Comparison of Drp1 Isoform 1's bulk fission rates in the presence of Mff revealed it to be slower than Drp1 Isoform 3 (Figure 5.2 B, blue dots indicate Isoform 1 fission rates, while red dots represent Isoform 3 fission rates). The analysis of percentage tubes cut revealed Drp1 Isoform 1 to be active but to a significantly lesser extent in comparison to Isoform 3 (data not shown). Thus, Drp1 Isoform 1 was fission defective in the presence of Mff coated supported membrane templates.

The defect in the fission might arise either due to a) a defect in the recruitment b) defect in the formation of higher order oligomer c) a defect in the GTPase activity or all of them. In order to distinguish the Drp1 Isoform 1's fission defect, mEGFP tag was engineered at its C-terminus (Drp1-mEGFP, Isoform 1). Interestingly, when equimolar mixture of Drp1 Isoform 1-mEGFP and Drp1 Isoform 1 was flown in the presence of GMP-PNP on Mff coated templates, it barely bound to the tubes and supported lipid bilayer (Figure 5.2 C). The defect in Drp1 Isoform 1 recruitment became apparent when it was compared to Drp1 Isoform 3 binding on Mff coated templates (Figure 5.2 D).

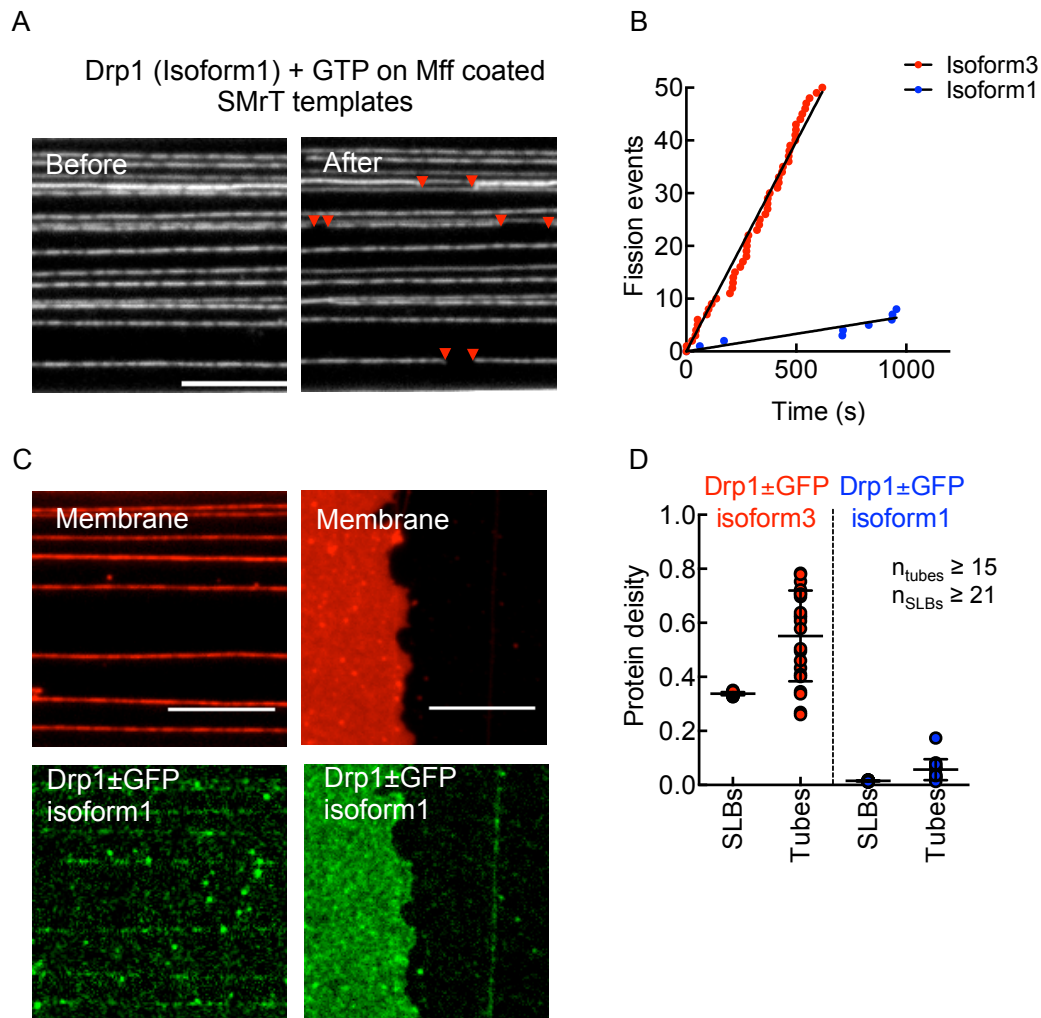


**Figure 5.2 Drp1 Isoform 1 is defective in membrane recruitment and fission on Mff coated supported membrane templates**

(A) Representative images of membrane tubes coated with Mff on flowing in Drp1 Isoform 1 and GTP (Membrane composition: DOPC:CL:DGS-NiNTA:*p*-TxRed DHPE 89:5:5:1 mol%). Red arrowhead in the after field marks the site for fission. Scale bar = 10 $\mu$ m. (B) Bulk fission rates in the presence of Mff coated templates on flowing in Drp1 Isoform 1 (Blue) and Drp1 Isoform 3 (Red) in the presence of GTP. (C) Representative images of Drp1±GFP (Isoform 1) on tubes and SLB with 5 mol% CL with Mff. Scale bar = 10 $\mu$ m. (D) Ratios of Drp1±GFP (Isoform 3 and Isoform 1) and the membrane fluorescence under GMP-PNP bound state on the SLB and tubes. The data represent mean  $\pm$  S.D; the number of tubes and SLBs analyzed is indicated by  $n_{\text{tubes}}$  and  $n_{\text{SLBs}}$  respectively.

### 5.3.2 Isoform 1 is defective in fission of CL-containing tubes

In order to investigate if Drp1 Isoform 1 is defective in binding to Mff or CL, a simpler system of 25 mol% cardiolipin without Mff was utilized. As shown in chapter 3, Drp1 Isoform 3 was able to sever membrane tubes containing 25 mol% CL. Surprisingly, Drp1 Isoform 1 was seen incapable of catalyzing membrane fission in

the same experimental conditions (Figure 5.3 A). While the other Drp1 Isoform, Isoform 2 was also able to catalyze membrane fission (Isoform 2 has 533-558 amino acid residues missing in the B-insert missing) (Figure 5.3 B).

This was also evident when number of tubes cut per field was analyzed, revealing Drp1 Isoform 1 to be severely defective in membrane fission (Figure 5.3 C). The comparison of membrane tube radii across experiments pointed out the fact that it was not significantly different thus negating the role of tube size on membrane fission (mentioned in panel above the stills).

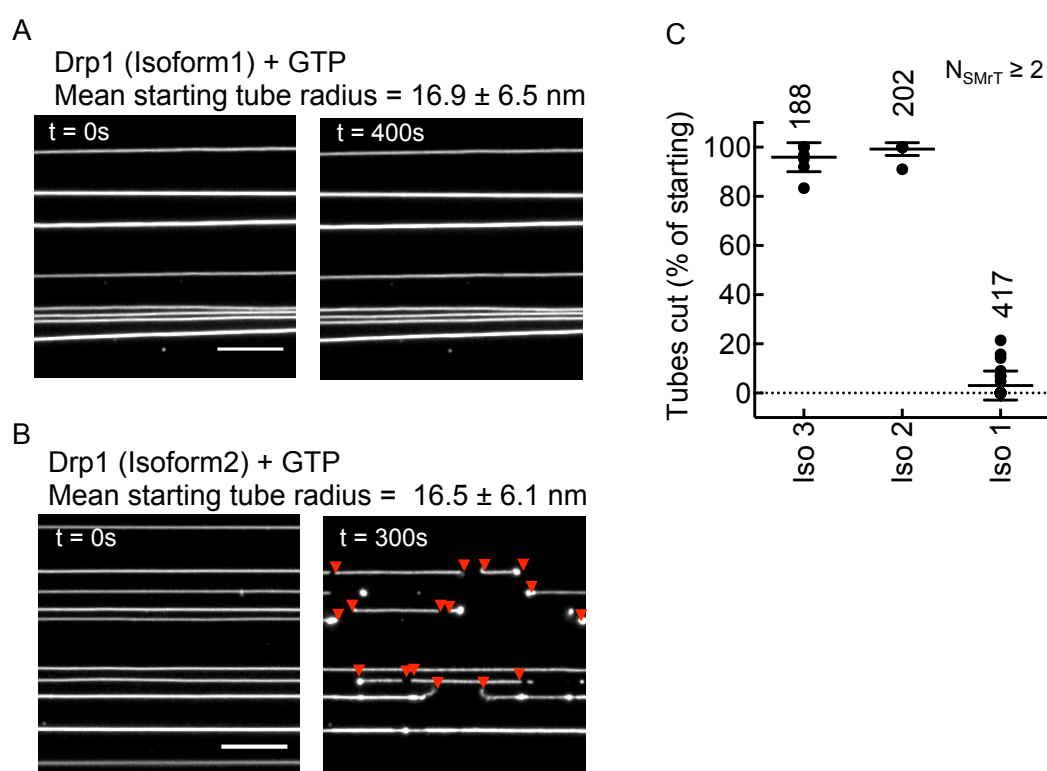


### Figure 5.3 Isoform 1 is defective in fission of CL-containing tubes

Stills from movies acquired while flowing in Drp1 Isoform 1 (A) and Isoform 2 (B), in the constant presence of GTP on 25 mol% CL containing membrane templates. Red arrowheads mark the site of fission. (Membrane composition DOPC:CL:*p*-TxRed DHPE 74:25:1 mol%). (C) Quantitation of fission events after flowing in different Drp1 Isoforms. The data represent mean  $\pm$  S.D; the total number of tubes analyzed across different fields is indicated above each data set. Each point in the data set represents an average number of tubes cut per field.

### **5.3.3 Isoform 1 is defective in binding cardiolipin-containing membranes despite possessing a functional B-insert**

In order to understand the defect in fission of Drp1 Isoform 1, GTPase assay was performed. In the absence of liposomes, Drp1 Isoform 1 displayed a basal GTPase activity of  $1.0 \pm 0.09 \mu\text{M Pi release}\cdot\text{min}^{-1}$ . Surprisingly, Drp1 Isoform 1 didn't show any stimulated GTPase activity in the presence of 25 mol% cardiolipin-containing liposomes (stimulated activity was  $1.9 \pm 0.12 \mu\text{M Pi release}\cdot\text{min}^{-1}$ ) (Figure 5.4 A). Given that Isoform 1 and 3 display similar basal GTPase activity, Drp1 Isoform 1 is unlikely to be defective in GTP hydrolysis. Impairment in the stimulated GTPase activity is instead suggestive of a defect in either membrane binding or assembly of Isoform 1. In order to test this hypothesis, Drp1±GFP (Isoform 1) was flown on 25 mol % CL containing supported membrane templates in the presence of different nucleotides. Drp1±GFP (Isoform 1) displayed poor recruitment to the membrane tubes (Figure 5.4 B), which became apparent when compared to Drp1±GFP (Isoform 3).

Since these Isoforms differs only in the B-insert region, it was argued if the defect in binding could arise from differential binding affinities of the B-inserts. However, the B-insert from Isoform 1 showed similar binding to the B-insert of Isoform 3 (Figure 5.4 C).



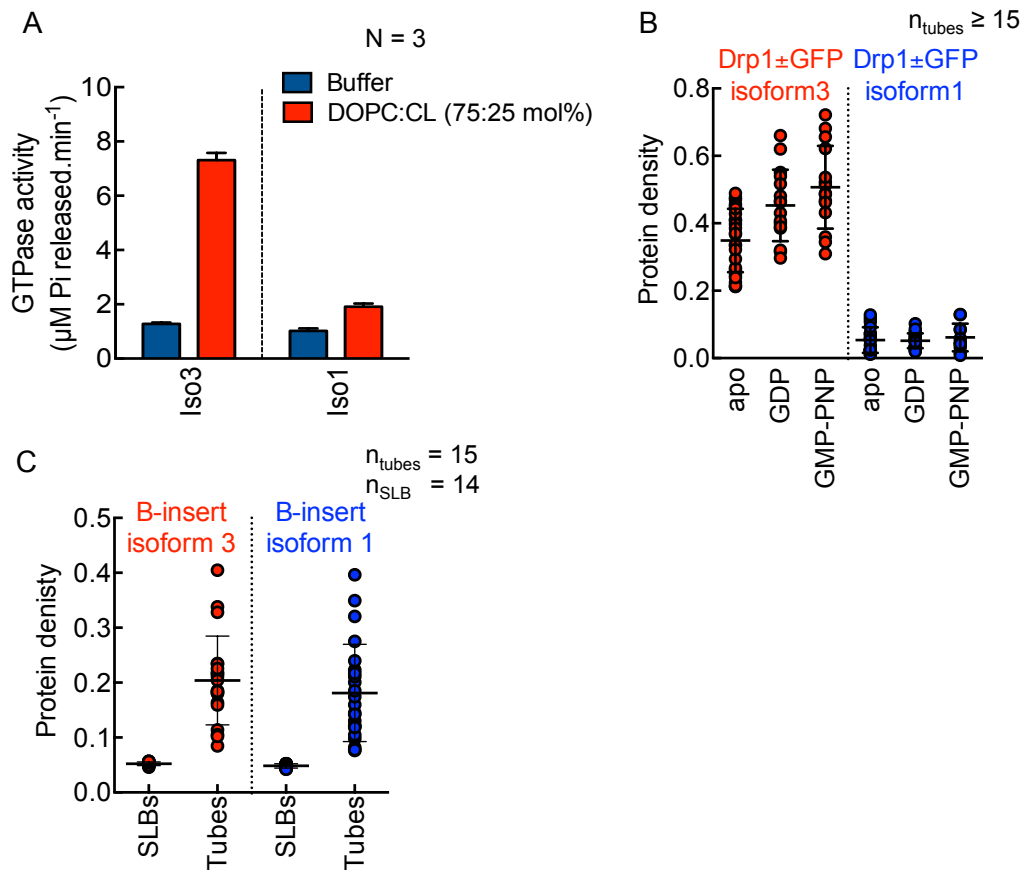


**Figure 5.4 Isoform 1 is defective in binding cardiolipin-containing membranes despite possessing a functional B-insert**

(A) GTPase assay with Drp1 Isoform 3 and 1. The data represent mean  $\pm$  S.D; N indicates the number of independent experiments performed. (B) Ratios of Drp1±GFP (Isoform 1 and Isoform 3) to the membrane fluorescence on tubes in the apo, GDP and GMP-PNP bound states. The data represent mean  $\pm$  S.D; number of tubes analyzed is indicated by  $n_{\text{tubes}}$ . (C) Ratio of GFP-Drp1-B-insert (Isoform 3 and Isoform 1) to the membrane fluorescence across SLBs and tubes. The data represent mean  $\pm$  S.D, number of tubes and SLBs analyzed is indicated by  $n_{\text{tubes}}$ ,  $n_{\text{SLBs}}$  respectively.

## Discussion

Although Drp1 is ubiquitously expressed, its Isoforms that are a result of alternative splicing, have a tissue-specific expression. Drp1 Isoform 1, which is the longest Isoform, is expressed explicitly in the brain, while Isoform 2 and 3 that are splice variants in the B-insert region are expressed in testis and skeletal muscles<sup>99</sup>. Surprisingly, although B-inserts of both the Isoforms showed a comparable binding to 25 mol% CL tubes, Drp1 Isoform 1 showed a drastically reduced fission activity (as compared to Isoform 2 and Isoform 3) on cardiolipin-containing tubes. Drp1 Isoform 1 displayed defect in membrane binding and consequently in stimulated GTPase

activity explaining the impairment in its ability to catalyze fission. Interestingly, Isoform 1 also showed reduced binding to- and impaired fission of Mff-coated tubes, highlighting the intrinsic differences in Drp1 Isoforms.

These results are consistent with the earlier cellular studies that reported Isoform 1 to only partially rescue normal mitochondrial morphology in Drp1 knockout background<sup>97</sup>. Also, it has been previously shown that the overexpression of Isoform 1 inhibits the peroxisomal fission<sup>100</sup>.

Studies indicate that the B-insert of Drp1 has an autoinhibitory role<sup>89,97,105</sup> and that the autoinhibition might get released on deletion of the B-insert, indicating that the B-insert apart from cardiolipin binding has a role to play in regulating Drp1's functions.

This inhibition might be a way for regulating Drp1 Isoform 1's fission activity, which may get relieved upon interaction with its cognate mitochondrial adaptor proteins displayed on the mitochondrial outer membrane. Alternatively, a possibility remains that Drp1 Isoform 1's fission activity is regulated by post-translational modification.

## Summary

Dynamin-related protein 1 (Drp1) is necessary for the mitochondrial division, but its precise involvement in the fission pathway remains unclear. The current model proposes cooperation between the mitochondrial and classical dynamins, and that neither alone is sufficient for mitochondrial fission. Using the facile SMrT system that comprises of membrane organized as curved tubes and planar sheet, mimicking the constricted and non-constricted states of the mitochondria, we find that Drp1 preferentially binds the tubes and is sufficient to catalyze their scission. Interestingly, the lipid-binding B-insert region in Drp1 also shows curvature preference of binding to the tubes as compared to planar bilayer thus augmenting Drp1's curvature sensing. Drp1 assembles in the form of scaffolds on membrane tubes in the presence of GTP, and upon hydrolysis causes their fission. The fission is robust, with Drp1 capable of catalyzing fission of tubes as wide as 500 nm. The fission process by Drp1 also seems to be evolutionarily conserved across the *drosophila* and *yeast* orthologs of Drp1.

Not all Drp1 foci on mitochondria are engaged in division<sup>39,106</sup>, thus suggesting the presence of an inhibitory signal to precisely control the site of fission. Such inhibitory signals may arise from the presence of specific mitochondrial lipids that regulate Drp1's function. Experimental evidence suggests that mitochondrial-division is inhibited in the presence of excess PA in the mitochondrial membrane<sup>76</sup>. The effect of PA on Drp1 function can be deciphered using SMrT modified to include PA in the membrane.

The presence of Drp1 adaptor proteins (Mff, MiD49, and MiD51) independently aids Drp1 recruitment and fission on the supported membrane templates. Indeed it is intriguing that Mff, MiD49 and MiD51 all co-localize at the site of mitochondrial division<sup>93</sup> given that each of them is sufficient to recruit Drp1<sup>88</sup>, suggesting an additional function for these adaptors in mitochondrial division. In this regards, Mff showed a unique tendency to oligomerize and cause membrane remodeling on tubes. Owing to this ability, Mff could potentially mark the site for mitochondrial division. Also, recently Kalia *et al.* reported a cryo-EM structure for the co-assembly of Drp1 and MiD49. Remarkably, upon GTP-hydrolysis Drp1 disassociated from MiD49 and formed ring-like intermediates<sup>24</sup>. Whether Mff and

MiD51 dissociate from Drp1 after its recruitment or are actively involved in the process of fission is still not known. The participation of these adaptor proteins in Drp1-mediated membrane fission can be tested using SMrT employing real-time fission analysis with fluorescently tagged constructs of Drp1 and the adaptor proteins. Another critical aspect would be to investigate the effect of adaptor proteins on the ability of Drp1 to catalyze fission of wide tubes.

A vast range of post-translational modifications play a major role in the regulation of mitochondrial fission<sup>8</sup>. Phosphorylation<sup>48,107-109</sup>, SUMOylation<sup>110</sup>, and ubiquitination<sup>111</sup> are known to regulate Drp1's function. In conjunction, the function of adaptor proteins is also regulated by post-translational modifications<sup>112</sup>. The individual contribution of these post-translational modifications on Drp1's activity can be deciphered using post-translationally modified/mimetic mutants of Drp1/adaptors using SMrTs.

Various Drp1 Isoforms are expressed differentially across cell-types<sup>99</sup>. The reason for this differential expression of the Isoform is still not known. Surprisingly, Drp1's longest Isoform; Isoform 1 is impaired in membrane binding and fission. This observation is in consensus with the cellular studies that indicate Isoform 1 only partially rescues mitochondrial morphology in the background of Drp1 knockdown<sup>97</sup>. Indeed, the individual contribution of each of these regulatory elements (presence of specific adaptors and/or lipids, post-translational modifications) to Drp1-mediated membrane fission can now be understood using the supported membrane templates.

## Manuscripts published

1. **Kamerkar, S.C\***, Kraus, F.\*, Sharpe, A.J., Pucadyil, T.J\*, and Ryan, M.T\*. Dynamin-related protein 1 has membrane constricting and severing abilities sufficient for mitochondrial and peroxisomal fission. *Nat. Commun.* 9, 5239 (2018).
2. **Kamerkar, S.C**, Roy, K., Bhattacharyya, S., and Pucadyil, T. A screen for membrane fission catalysts identifies the ATPase EHD1. *Biochemistry*. DOI: 10.1021/acs.biochem.8b00925. (2018).
3. Deo, R.\*, Kushwah, M.S.\*, **Kamerkar, S.C.**, Kadam, N.Y., Dar, S., Babu, K., Srivastava, A., and Pucadyil, T.J. ATP-dependent membrane remodeling links EHD1 functions to endocytic recycling. *Nat. Commun.* 9, 5187. (2018).
4. Singh, P.K., Kapoor, A., Lomash, R.M., Kumar, K., **Kamerkar, S.C.**, Pucadyil, T.J., and Mukhopadhyay, A. Salmonella SipA mimics a cognate SNARE for host Syntaxin8 to promote fusion with early endosomes. *J. Cell Biol.* 217, 4199–4214. (2018).
5. Dar, S., **Kamerkar, S. C.** and Pucadyil, T. J. Use of the supported membrane tube assay system for real-time analysis of membrane fission reactions. *Nature Protocols* 12, 390–400 (2017).
6. Dar, S., **Kamerkar, S. C.** and Pucadyil, T. J. A high-throughput platform for real-time analysis of membrane fission reactions reveals dynamin function. *Nature Cell Biology* 17, 1588-1596 (2015).
7. Holkar, S. S., **Kamerkar, S. C.** and Pucadyil, T. J. Spatial control of epsin induced clathrin assembly by membrane curvature. *Journal of Biological Chemistry* 290, 14267–14276 (2015).

## References

1. Youle, R. J. & Van Der Bliek, A. M. Mitochondrial fission, fusion, and stress. *Science*. **337**, 1062–1065 (2012).
2. Gray, M. W., Burger, G. & Lang, F. Mitochondrial evolution. *Science*. **283**, 1476–1481 (1999).
3. Plattner, H., Salpeter, M. M., Saltzgaber, J. & Schatz, G. Promitochondria of anaerobically grown yeast. IV. Conversion into respiring mitochondria. *Proc. Natl. Acad. Sci. U. S. A.* **66**, 1252–1259 (1970).
4. Twig, G. *et al.* Fission and selective fusion govern mitochondrial segregation and elimination by autophagy. *EMBO J.* **27**, 433–446 (2008).
5. Martinou, J. C. & Youle, R. J. Mitochondria in Apoptosis: Bcl-2 Family Members and Mitochondrial Dynamics. *Dev. Cell* **21**, 92–101 (2011).
6. Chan, D. C. Mitochondrial fusion and fission in mammals. *Annu. Rev. Cell Dev. Biol.* **22**, 79–99 (2006).
7. Westermann, B. Mitochondrial dynamics in model organisms: What yeasts, worms and flies have taught us about fusion and fission of mitochondria. *Semin. Cell Dev. Biol.* **21**, 542–549 (2010).
8. van der Bliek, A. M., Shen, Q. & Kawajiri, S. Mechanisms of mitochondrial fission and fusion. *Cold Spring Harb. Perspect. Biol.* **5**, (2013).
9. Smirnova, E., Shurland, D.-L., Ryazantsev, S. N. & Van der Bliek, A. M. A human dynamin-related protein controls the distribution of mitochondria. *J. Cell Biol.* **143**, 351–358 (1998).
10. Smirnova, E., Griparic, L., Shurland, D. & Bliek, A. M. Van Der. Dynamin-related Protein Drp1 Is Required for Mitochondrial Division in Mammalian Cells. *Mol. Biol. Cell* **12**, 2245–2256 (2001).
11. Friedman, J. R. *et al.* ER tubules mark sites of mitochondrial division. *Science* **334**, 358–62 (2011).
12. Pagliuso, A., Cossart, P. & Stavru, F. The ever-growing complexity of the mitochondrial fission machinery. *Cell. Mol. Life Sci.* **75**, 355–374 (2018).
13. Lee, J. E., Westrate, L. M., Wu, H., Page, C. & Voeltz, G. K. Multiple dynamin family members collaborate to drive mitochondrial division. *Nature* **540**, 139–

- 143 (2016).
14. Fujioka, H., Tandler, B. & Hoppel, C. L. Mitochondrial Division in Rat Cardiomyocytes: An Electron Microscope Study. *Anat. Rec.* **295**, 1455–1461 (2012).
  15. Wakabayashi, J. *et al.* The dynamin-related GTPase Drp1 is required for embryonic and brain development in mice. *J. Cell Biol.* **186**, 805–816 (2009).
  16. Ishihara, N. *et al.* Mitochondrial fission factor Drp1 is essential for embryonic development and synapse formation in mice. *Nat. Cell Biol.* **11**, 958–966 (2009).
  17. Koch, A. *et al.* Dynamin-like protein 1 is involved in peroxisomal fission. *J. Biol. Chem.* **278**, 8597–8605 (2003).
  18. Smith, J. J. & Aitchison, J. D. Peroxisomes take shape. *Nat. Rev. Mol. Cell Biol.* **14**, 803–817 (2013).
  19. Fröhlich, C. *et al.* Structural insights into oligomerization and mitochondrial remodelling of dynamin 1-like protein. *EMBO J.* **32**, 1280–92 (2013).
  20. Liu, R. & Chan, D. C. The mitochondrial fission receptor Mff selectively recruits oligomerized Drp1. *Mol. Biol. Cell* **26**, 4466–4477 (2015).
  21. Mears, J. a *et al.* Conformational changes in Dnm1 support a contractile mechanism for mitochondrial fission. *Nat. Struct. Mol. Biol.* **18**, 20–26 (2011).
  22. Ingeman, E. *et al.* Dnm1 forms spirals that are structurally tailored to fit mitochondria. *J. Cell Biol.* **170**, 1021–1027 (2005).
  23. Basu, K. *et al.* Molecular mechanism of DRP1 assembly studied in vitro by cryo-electron microscopy. 1–21 (2017).
  24. Kalia, R. *et al.* Structural basis of mitochondrial receptor binding and constriction by DRP1. *Nature* **558**, 401–405 (2018).
  25. Macdonald, P. J. *et al.* A dimeric equilibrium intermediate nucleates Drp1 reassembly on mitochondrial membranes for fission. *Mol. Biol. Cell* **25**, 1905–15 (2014).
  26. Ugarte-Uribe, B., Müller, H.-M., Otsuki, M., Nickel, W. & García-Sáez, A. J. Dynamin-related Protein 1 (Drp1) Promotes Structural Intermediates of Membrane Division. *J. Biol. Chem.* **289**, 30645–56 (2014).
  27. Ugarte-Uribe, B., Prévost, C., Das, K. K., Bassereau, P. & García-Sáez, A. J. Drp1 polymerization stabilizes curved tubular membranes similar to those of

- constricted mitochondria. *J. Cell Sci.* **132**, jcs208603 (2017).
28. Bui, H. T. & Shaw, J. M. Dynamin assembly strategies and adaptor proteins in mitochondrial fission. *Curr. Biol.* **23**, R891–R899 (2013).
  29. Mozdy, A. D., McCaffery, J. M. & Shaw, J. M. Dnm1p GTPase-mediated mitochondrial fission is a multi-step process requiring the novel integral membrane component Fis1p. *J. Cell Biol.* **151**, 367–379 (2000).
  30. Otera, H. *et al.* Mff is an essential factor for mitochondrial recruitment of Drp1 during mitochondrial fission in mammalian cells. *J. Cell Biol.* **191**, 1141–1158 (2010).
  31. Lee, Y., Jeong, S., Karbowski, M., Smith, C. L. & Youle, R. J. Roles of the Mammalian Mitochondrial Fission and Fusion Mediators Fis1, Drp1, and Opa1 in Apoptosis. **15**, 5001–5011 (2004).
  32. Gandre-Babbe, S. & Van der Bliek, A. M. The Novel Tail-anchored Membrane Protein Mff Controls Mitochondrial and Peroxisomal Fission in Mammalian Cells. *Mol. Biol. Cell* **19**, 308–317 (2007).
  33. Friedman, J. R. *et al.* ER tubules mark sites of mitochondrial division. *Science.* **334**, 358–362 (2011).
  34. Waterham, H. R. *et al.* A Lethal Defect of Mitochondrial and Peroxisomal Fission. *N. Engl. J. Med.* **356**, 1736–1741 (2007).
  35. Palmer, C. S. *et al.* MiD49 and MiD51, new components of the mitochondrial fission machinery. *EMBO Rep.* **12**, 565–573 (2011).
  36. Zhao, J. *et al.* Human MIEF1 recruits Drp1 to mitochondrial outer membranes and promotes mitochondrial fusion rather than fission. *EMBO J.* **30**, 2762–2778 (2011).
  37. Copeland, D. E. An Association between Mitochondria and the Endoplasmic Reticulum in Cells of the Pseudobranch Gland of a Teleost. *J. Cell Biol.* **5**, 393–396 (1959).
  38. Elgass, K. D., Smith, E. A., LeGros, M. A., Larabell, C. A. & Ryan, M. T. Analysis of ER-mitochondria contacts using correlative fluorescence microscopy and soft X-ray tomography of mammalian cells. *J. Cell Sci.* **128**, 2795–2804 (2015).
  39. Ji, W. K., Hatch, A. L., Merrill, R. A., Strack, S. & Higgs, H. N. Actin filaments target the oligomeric maturation of the dynamin GTPase Drp1 to



- mitochondrial fission sites. *Elife* **4**, 1–25 (2015).
40. Manor, U. *et al.* A mitochondria-anchored isoform of the actin-nucleating spire protein regulates mitochondrial division. *Elife* **4**, 1–27 (2015).
  41. Korobova, F., Gauvin, T. J. & Higgs, H. N. A role for myosin II in mammalian mitochondrial fission. *Curr. Biol.* **24**, 409–414 (2014).
  42. Moore, A. S., Wong, Y. C., Simpson, C. L. & Holzbaur, E. L. F. Dynamic actin cycling through mitochondrial subpopulations locally regulates the fission-fusion balance within mitochondrial networks. *Nat. Commun.* **7**, 1–13 (2016).
  43. Pagliuso, A. *et al.* Mitochondrial Fission. *EMBO Rep.* **17**, 1–16 (2016).
  44. Martorell Riera, A. *et al.* Dynamin-2 facilitates Atg9 recycling from nascent autophagosomes. *bioRxiv* [https://doi](https://doi.org/10.1101/2018.08.14.241111), (2018).
  45. Kamerkar, S. C., Kraus, F., Sharpe, A. J., Pucadyil, T. J. & Ryan, M. T. Dynamin-related protein 1 has membrane constricting and severing abilities sufficient for mitochondrial and peroxisomal fission. *Nat. Commun.* **9**, 5239 (2018).
  46. Collins, T. J., Berridge, M. J., Lipp, P. & Bootman, M. D. Mitochondria are morphologically and functionally heterogeneous within cells. *EMBO J.* **21**, 1616–1627 (2002).
  47. Westermann, B. Bioenergetic role of mitochondrial fusion and fission. *Biochim. Biophys. Acta - Bioenerg.* **1817**, 1833–1838 (2012).
  48. Taguchi, N., Ishihara, N., Jofuku, A., Oka, T. & Mihara, K. Mitotic phosphorylation of dynamin-related GTPase Drp1 participates in mitochondrial fission. *J. Biol. Chem.* **282**, 11521–11529 (2007).
  49. Labbé, K., Murley, A. & Nunnari, J. Determinants and Functions of Mitochondrial Behavior. *Annu. Rev. Cell Dev. Biol.* **30**, 357–391 (2014).
  50. Lackner, L. L. Determining the shape and cellular distribution of mitochondria: The integration of multiple activities. *Curr. Opin. Cell Biol.* **25**, 471–476 (2013).
  51. Chen, H. & Chan, D. C. Mitochondrial dynamics-fusion, fission, movement, and mitophagy-in neurodegenerative diseases. *Hum. Mol. Genet.* **18**, 169–176 (2009).
  52. Smirnova, E., Shurland, D. L., Ryazantsev, S. N. & Van Der Bliek, A. M. A

- human dynamin-related protein controls the distribution of mitochondria. *J. Cell Biol.* **143**, 351–358 (1998).
53. Dar, S., Kamerkar, S. C. & Pucadyil, T. J. Use of the supported membrane tube assay system for real-time analysis of membrane fission reactions. *Nat. Protoc.* **12**, 390–400 (2017).
  54. Hu, G. Bin. Whole cell cryo-electron tomography suggests mitochondria divide by budding. *Microsc. Microanal.* **20**, 1180–1187 (2014).
  55. Jung, H., Robison, A. D. & Cremer, P. S. Detecting protein-ligand binding on supported bilayers by local pH modulation. *J. Am. Chem. Soc.* **131**, 1006–1014 (2009).
  56. Pucadyil, T. J. & Holkar, S. S. Comparative analysis of adaptor-mediated clathrin assembly reveals general principles for adaptor clustering. *Mol. Biol. Cell* **27**, 3156–3163 (2016).
  57. Dar, S. & Pucadyil, T. J. The pleckstrin-homology domain of dynamin is dispensable for membrane constriction and fission. *Mol. Biol. Cell* **28**, 152–160 (2017).
  58. Hatzakis, N. S. *et al.* How curved membranes recruit amphipathic helices and protein anchoring motifs. *Nat. Chem. Biol.* **5**, 835–41 (2009).
  59. Petit, Jean-Michel, Abderrahman MAFTAH, M.-H. R. and R. J. Institut. 1ON-Nonyl acridine orange interacts with cardiolipin and allows the quantification. *FEBS Lett.* **273**, 267–273 (1992).
  60. Schindelin, J. *et al.* Fiji: an open-source platform for biological-image analysis. *Nat. Methods* **9**, 676–682 (2012).
  61. Karbowski, M. & Youle, R. J. Dynamics of mitochondrial morphology in healthy cells and during apoptosis. *Cell Death Differ.* **10**, 870–80 (2003).
  62. Westermann, B. Mitochondrial fusion and fission in cell life and death. *Nat. Rev. Mol. Cell Biol.* **11**, 872–884 (2010).
  63. Holkar, S. S., Kamerkar, S. C. & Pucadyil, T. J. Spatial control of epsin-induced clathrin assembly by membrane curvature. *J. Biol. Chem.* **290**, 14267–14276 (2015).
  64. Dar, S., Kamerkar, S. C. & Pucadyil, T. J. A high-throughput platform for real-time analysis of membrane fission reactions reveals dynamin function. *Nat. Cell Biol.* **17**, 1588–1596 (2015).

65. Dragsten, P. R., Blumenthal, R. & Handler, J. S. Membrane asymmetry in epithelia: Is the tight junction a barrier to diffusion in the plasma membrane? *Nature* **294**, 718–722 (1981).
66. Melikyan, G. B., Deriy, B. N., Ok, D. C. & Cohen, F. S. Voltage-dependent translocation of R18 and Dil across lipid bilayers leads to fluorescence changes. *Biophys. J.* **71**, 2680–2691 (1996).
67. Zinser, E. *et al.* Phospholipid synthesis and lipid composition of subcellular membranes in the unicellular eukaryote *Saccharomyces cerevisiae*. *J. Bacteriol.* **173**, 2026–2034 (1991).
68. Comte, j., maisterrena, b. & gautheron, d. Lipid composition and protein profiles of outer and inner membranes from pig heart mitochondria comparison with microsomes. *Biochim. Biophys. Acta* **7**, 271–284 (1976).
69. Van Meer, G., Voelker, D. R. & Feigenson, G. W. Membrane lipids: Where they are and how they behave. *Nat. Rev. Mol. Cell Biol.* **9**, 112–124 (2008).
70. Daum, G. Lipids of mitochondria. *Biochim. Biophys. Acta - Rev. Biomembr.* **822**, 1–42 (1985).
71. Ardail, D. *et al.* Mitochondrial Contact Sites. *J. Biol. Chem.* **265**, (1990).
72. Schlattner, U. *et al.* Mitochondrial cardiolipin/phospholipid trafficking: The role of membrane contact site complexes and lipid transfer proteins. *Chem. Phys. Lipids* **179**, 32–41 (2014).
73. Tatsuta, T., Scharwey, M. & Langer, T. Mitochondrial lipid trafficking. *Trends Cell Biol.* **24**, 44–52 (2014).
74. Sorice, M. *et al.* Cardiolipin-enriched raft-like microdomains are essential activating platforms for apoptotic signals on mitochondria. *FEBS Lett.* **583**, 2447–2450 (2009).
75. Bustillo-Zabalbeitia, I. *et al.* Specific Interaction with Cardiolipin Triggers Functional Activation of Dynamin-Related Protein 1. *PLoS One* **9**, e102738 (2014).
76. Adachi, Y. *et al.* Coincident Phosphatidic Acid Interaction Restrains Drp1 in Mitochondrial Division. *Mol. Cell* **63**, 1034–1043 (2016).
77. Francy, C. A., Alvarez, F. J. D., Zhou, L., Ramachandran, R. & Mears, J. A. The mechanoenzymatic core of dynamin-related protein 1 comprises the minimal machinery required for membrane constriction. *J. Biol. Chem.* **290**,

- 11692–11703 (2015).
78. Bubeck, P., Winkler, M. & Bautsch, W. Rapid cloning by homologous recombination in vivo. *Nucleic Acids Res.* **21**, 3601–2 (1993).
  79. Baykov, A. A. A Malachite Green Procedure for Orthophosphate Determination and Its Use in Alkaline Phosphatase-Based Enzyme Immunoassay. *Anal. Biochem.* **270**, 266–270 (1988).
  80. Salim, K. *et al.* Distinct specificity in the recognition of phosphoinositides by the pleckstrin homology domains of dynamin and Bruton 's tyrosine kinase. *EMBO J.* **15**, 6241–6250 (1996).
  81. Chang, C. R. *et al.* A lethal de novo mutation in the middle domain of the dynamin-related GTPase Drp1 impairs higher order assembly and mitochondrial division. *J. Biol. Chem.* **285**, 32494–32503 (2010).
  82. Korobova, F., Ramabhadran, V. & Higgs, H. N. An actin-dependent step in mitochondrial fission mediated by the ER-associated formin INF2. *Science.* **339**, 464–467 (2013).
  83. Hatch, A. L., Ji, W.-K., Merrill, R. A., Strack, S. & Higgs, H. N. Actin filaments as dynamic reservoirs for Drp1 recruitment. *Mol. Biol. Cell* **27**, 3109–3121 (2016).
  84. Iversen, T.-G., Skretting, G., van Deurs, B. & Sandvig, K. Clathrin-coated pits with long, dynamin-wrapped necks upon expression of a clathrin antisense RNA. *Proc. Natl. Acad. Sci.* **100**, 5175–80 (2003).
  85. Wu, H., Carvalho, P. & Voeltz, G. K. Here, there, and everywhere: The importance of ER membrane contact sites. *Rev. Summ. Cell Biol.* **466**, (2018).
  86. Loson, O. C., Song, Z., Chen, H. & Chan, D. C. Fis1, Mff, MiD49, and MiD51 mediate Drp1 recruitment in mitochondrial fission. *Mol. Biol. Cell* **24**, 659–667 (2013).
  87. Palmer, C. S. *et al.* Adaptor proteins MiD49 and MiD51 can act independently of Mff and Fis1 in Drp1 recruitment and are specific for mitochondrial fission. *J. Biol. Chem.* **288**, 27584–27593 (2013).
  88. Koirala, S. *et al.* Interchangeable adaptors regulate mitochondrial dynamin assembly for membrane scission. *Proc. Natl. Acad. Sci.* **110**, E1342–E1351 (2013).
  89. Strack, S. & Cribbs, J. T. Allosteric modulation of Drp1 mechanoenzyme

- assembly and mitochondrial fission by the variable domain. *J. Biol. Chem.* **287**, 10990–1001 (2012).
90. Richter, V. *et al.* Structural and functional analysis of mid51, a dynamin receptor required for mitochondrial fission. *J. Cell Biol.* **204**, 477–486 (2014).
  91. Losón, O. C. *et al.* Crystal structure and functional analysis of MiD49, a receptor for the mitochondrial fission protein Drp1. *Protein Sci.* **24**, 386–394 (2015).
  92. Helle, S. C. J. *et al.* Mechanical force induces mitochondrial fission. *Elife* **6**, 1–26 (2017).
  93. Osellame, L. D. *et al.* Cooperative and independent roles of the Drp1 adaptors Mff, MiD49 and MiD51 in mitochondrial fission. *J. Cell Sci.* **129**, 2170–2181 (2016).
  94. Kraus, F. & Ryan, M. T. The constriction and scission machineries involved in mitochondrial fission. *J. Cell Sci.* **130**, 2953–2960 (2017).
  95. Horvath, S. E. & Daum, G. Lipids of mitochondria. *Prog. Lipid Res.* **52**, 590–614 (2013).
  96. Losón, O. C. *et al.* The mitochondrial fission receptor MiD51 requires ADP as a cofactor. *Structure* **22**, 367–377 (2014).
  97. Clinton, R. W., Francy, C. A., Ramachandran, R., Qi, X. & Mears, J. A. Dynamin-related protein 1 oligomerization in solution impairs functional interactions with membrane-anchored mitochondrial fission factor. *J. Biol. Chem.* **291**, 478–492 (2016).
  98. Lewis, T. L., Kwon, S.-K., Lee, A., Shaw, R. & Polleux, F. MFF-dependent mitochondrial fission regulates presynaptic release and axon branching by limiting axonal mitochondria size. *Nat. Commun.* (2018). doi:10.1101/276691
  99. Kamimoto, T. *et al.* Dymple, a novel dynamin-like high molecular weight GTPase lacking a proline-rich carboxyl-terminal domain in mammalian cells. *J. Biol. Chem.* **273**, 1044–1051 (1998).
  100. Li, X. & Gould, S. J. The dynamin-like GTPase DLP1 is essential for peroxisome division and is recruited to peroxisomes in part by PEX11. *J. Biol. Chem.* **278**, 17012–17020 (2003).
  101. Strack, S., Wilson, T. J. & Cribbs, J. T. Cyclin-dependent kinases regulate splice-specific targeting of dynamin-related protein 1 to microtubules. *J. Cell*

- Biol.* **201**, 1037–1051 (2013).
102. Itoh, K. *et al.* A brain-enriched drp1 isoform associates with lysosomes, late endosomes, and the plasma membrane. *J. Biol. Chem.* **293**, 11809–11822 (2018).
  103. Consortium, T. U. UniProt : the universal protein knowledgebase. *Nucleic Acids Res.* **45**, 158–169 (2017).
  104. Larkin, M. A. *et al.* Clustal W and Clustal X version 2 . 0. *bioinformatics* **23**, 2947–2948 (2007).
  105. Lu, B. *et al.* Steric interference from intrinsically disordered regions controls dynamin-related protein 1 self-assembly during mitochondrial fission. *Sci. Rep.* **8**, 1–21 (2018).
  106. Roy, M., Reddy, P. H., Iijima, M. & Sesaki, H. Mitochondrial division and fusion in metabolism. *Curr. Opin. Cell Biol.* **33**, 111–118 (2015).
  107. Han, X. J. *et al.* CaM kinase I $\alpha$ -induced phosphorylation of Drp1 regulates mitochondrial morphology. *J. Cell Biol.* **182**, 573–585 (2008).
  108. Chang, C. R. & Blackstone, C. Dynamic regulation of mitochondrial fission through modification of the dynamin-related protein Drp1. *Ann. N. Y. Acad. Sci.* **1201**, 34–39 (2010).
  109. Chou, C. H. *et al.* GSK3 $\beta$ -Mediated Drp1 Phosphorylation Induced Elongated Mitochondrial Morphology against Oxidative Stress. *PLoS One* **7**, (2012).
  110. Braschi, E., Zunino, R. & McBride, H. M. MAPL is a new mitochondrial SUMO E3 ligase that regulates mitochondrial fission. *EMBO Rep.* **10**, 748–754 (2009).
  111. Karbowski, M., Neutzner, A. & Youle, R. J. The mitochondrial E3 ubiquitin ligase MARCH5 is required for Drp1 dependent mitochondrial division. *J. Cell Biol.* **178**, 71–84 (2007).
  112. Toyama, E. Q. *et al.* AMP-activated protein kinase mediates mitochondrial fission in response to energy stress. *Science.* **351**, 275–281 (2016).